FUEL EFFICIENCY BENEFITS AND IMPLEMENTATION CONSIDERATIONS FOR CRUISE ALTITUDE AND SPEED OPTIMIZATION IN THE NATIONAL AIRSPACE SYSTEM

Luke L. Jensen and R. John Hansman

This report is based on the Masters Thesis of Luke L. Jensen submitted to the Department of Aeronautics and Astronautics in partial fulfillment of the requirements for the degree of Master of Science at the Massachusetts Institute of Technology.

Report No. ICAT-2014-04
May 2014

MIT International Center for Air Transportation (ICAT)
Department of Aeronautics & Astronautics
Massachusetts Institute of Technology
Cambridge, MA 02139 USA

Page Intentionally Left Blank

FUEL EFFICIENCY BENEFITS AND IMPLEMENTATION CONSIDERATIONS FOR CRUISE ALTITUDE AND SPEED OPTIMIZATION IN THE NATIONAL AIRSPACE SYSTEM

by

Luke L. Jensen

Submitted to the Department of Aeronautics and Astronautics
on May 22, 2014, in partial fulfillment of the
requirements for the degree of
Master of Science in Aeronautics and Astronautics

ABSTRACT

This study examines the potential fuel burn benefits of altitude and speed optimization in the cruise phase of flight for domestic airlines in the United States. Airlines can achieve cost reductions and reduce environmental impact by making small modifications to the cruise phase operating condition. The efficiency of the National Airspace System can be improved with coordination between air traffic controllers, pilots, and airline dispatchers. This study builds off of prior work in this area to establish best-case benefits assuming full implementation of fuel-optimal cruise altitudes and speeds.

In order to achieve these objectives, a cruise-phase fuel burn estimator was developed using publicly-available radar tracks and weather data. This estimator was used to examine 217,000 flights from 2012. Maximum benefits from altitude optimization (holding speed constant) were found to be on the order 1.96%. The majority of potential altitude benefits can be achieved using step climb optimization, with only marginal gain from cruise climb implementation. The maximum benefits for speed optimization (holding altitude constant) were found to be 1.94% with an average flight time increase of 3.5 minutes per flight. Simultaneous altitude and speed optimization yielded a potential cruise fuel burn reduction of 3.71%. In practice, operational considerations and barriers to implementation limit likely system fuel reduction to lower levels. High-benefit operations within the NAS are identified and potential implementation considerations are discussed.

Thesis Supervisor: Dr. R. John Hansman
Title: T. Wilson Professor of Aeronautics and Astronautics

Page Intentionally Left Blank

ACKNOWLEDGEMENTS

First, I wish to thank Professor Hansman for his practical and academic guidance rooted in years of experience in aviation and engineering. Such perspective is immensely valuable for a graduate researcher and a student of aviation.

Second, I am thankful for the support of my collaborators at MIT Lincoln Laboratory (including Tom Reynolds, Joe Venuti, Alan Midkiff, and Yari Rodriguez) and project managers at the FAA AEE (including Pat Moran and Chris Dorbian). Collectively, their weekly feedback kept my research and analysis ideas on track.

I wish to acknowledge the long chain of teachers and mentors who have helped me grow academically and personally to meet the present challenge. Each new experience builds on the foundation of what comes before. I especially thank my teachers at the Bainbridge Island Public Schools, my mentors at the Port Townsend Aero Museum, and my professors at the University of Washington.

I am grateful for my year of travel between 2011 and 2012 and the impact it had on my present outlook toward academics and life. To all of the people I met on the road in all corners of the world, I pass along a heartfelt thanks. What goes around comes around.

Last, but certainly not least, I wish to thank my parents and my brother for being supportive throughout the journey that brought me here. Blue skies!

DISCLAIMER

This work was sponsored by the Federal Aviation Administration (FAA) under Air Force Contract FA8721-05-C-0002. Opinions, interpretations, conclusions, and recommendations are those of the author and are not necessarily endorsed by the United States Government.

Page Intentionally Left Blank

TABLE OF CONTENTS

LIST OF FIGURES

LIST OF TABLES

Page Intentionally Left Blank

ACRONYMS AND ABBREVIATIONS

ACARS	Aircraft Communications Addressing and Reporting System
AOA	Angle of Attack
ATC	Air Traffic Control
CASO	Cruise Altitude and Speed Optimization
CONUS	Continental United States
EDCT	Expected Departure Clearance Time
ETMS	Enhanced Traffic Management System
FAA	Federal Aviation Administration
FL	Flight Level
FMC	Flight Management Computer
GA	General Aviation
GDP	Ground Delay Program
LRC	Long Range Cruise Speed
MGTOW	Maximum Gross Takeoff Weight
MRC	Maximum Range Cruise Speed
NARR	North American Regional Reanalysis
NAS	National Airspace System
NOAA	National Oceanographic and Atmospheric Administration
PDF	Probability Density Function
PIREP	Pilot Report
RVSM	Reduced Vertical Separation Minima
SAR	Specific Air Range
SGR	Specific Ground Range
TOCW	Top-of-Climb Weight
TOW	Take Off Weight
VNAV	Vertical Navigation

Page Intentionally Left Blank

Chapter 1 INTRODUCTION

1.1 Motivation

This study examines the potential fuel burn benefits of altitude and speed optimization in the cruise phase of flight for domestic airlines in the United States. Airlines can achieve cost reductions and mitigate environmental impact by making small modifications to the cruise phase operating condition. With coordination between air traffic controllers, pilots, and airline dispatchers, the efficiency of the National Airspace System can be improved. This study builds off of prior work in this area to establish best-case benefits. High-benefit operations within the NAS are identified and potential implementation considerations are discussed. In order to achieve these objectives, a cruise-phase fuel burn estimator is developed using publicly-available radar tracks and weather data. This estimator is used to examine 217,000 flights from 2012 for optimization potential.

For airlines in the United States, fuel has become the largest component of operating costs [1]. In 2013, fuel costs for domestic operations alone totaled $31.1 billion [2]. Airlines worldwide spent about $211 billion on fuel accounting for 31% of all operational costs [3]. Despite newer aircraft types and engine technology entering the fleet, the unit cost for a gallon of fuel has risen by a factor of three over the span of a decade as shown in Figure 1. The growth and volatility of this major cost driver has led to increased focus on fuel conservation from stakeholders throughout the air transportation system.

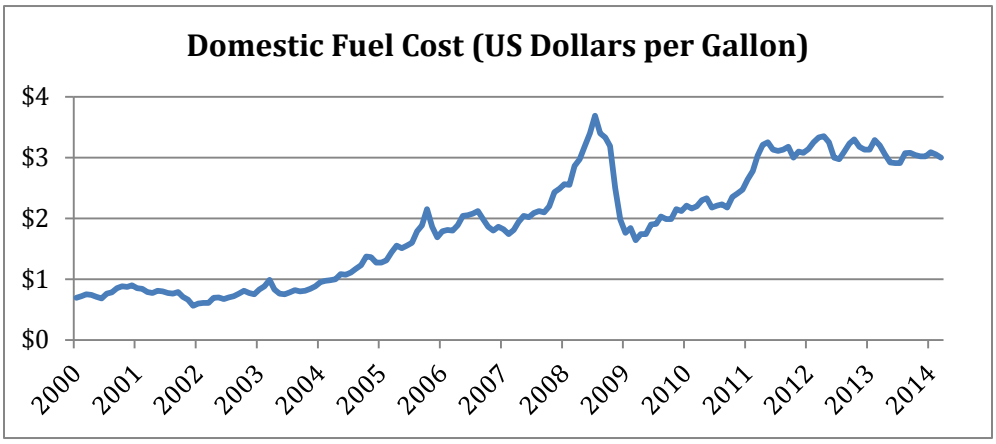

Figure 1. Average domestic US fuel price since 2000 (Source: RITA/BTS)

Environmental concerns provide further motivation for fuel conservation as climate and air-quality impacts from hydrocarbon fuel combustion gain greater scientific and social prominence. There are various techniques to control fuel-related environmental impact with

varying implementation timelines and potential benefit. These include new aircraft technology (decade-scale implementation, high cost), retrofits to existing aircraft technology (multi-year implementation, medium cost), alternative jet fuel and propulsion technology (decade-scale implementation, high cost), and operational mitigation (rapid implementation, low cost) [4]. Operational mitigations are useful due to the potential for rapid implementation and low capital expenditure, although the long-term benefit is generally less than other technology-driven solutions. Prior work in academia and industry has identified many potential operational mitigations, including barriers to implementation and potential benefits.

Operational strategies for fuel burn reduction are those that involve the manner in which an aircraft is flown, handled on the ground, or managed in the air traffic control (ATC) system. They are implementable without modification to aircraft structures or engines, but may require investment in avionics, infrastructure, and training. Operational mitigations can be implemented in all phases of flight. High-profile examples of operational strategies include single-engine taxi, continuous climb procedures, wind-optimal routing, and continuous descent approaches [5]. In the cruise phase of flight, one of the most promising operational opportunities in current operations and future trajectory-based operational frameworks is cruise altitude and speed optimization (CASO) given fixed lateral tracks. In order to understand the full potential of the concept and its implementation, extensive simulations and analysis are required.

Of all phases of flight, cruise optimization has particularly strong potential to increase efficiency in the National Airspace System. Based on the analysis conducted for this project, cruise operations account for an average of 56% of total flight time for all operations logged by the FAA Enhanced Traffic Management System (ETMS) in 2012 [6]. Globally, 85-90% of air transportation fuel consumption occur in high-altitude flight above 10,000 feet [7]. Improvements to cruise efficiency can have a large impact on the total system fuel consumption. While the advantage of reducing lateral track distance is clear, airspace constraints increase the complexity of implementation for this type of optimization. Another possible improvement involves adjustment of speed and/or altitude to reach optimal cruise conditions given a fixed lateral track.

The efficiency of an aircraft at any point along its flight path is a function of weight, altitude, speed, wind, temperature, and other second-order effects. At a fixed weight, there exists a combination of speed and altitude at which instantaneous fuel efficiency is maximized. Actual operating conditions may differ from this optimal point for a variety of operational and practical reasons. Figure 2 shows the impact of altitude and speed on fuel efficiency for a typical narrowbody airliner, measured in distance flown over the ground per unit of fuel (Specific Ground Range, SGR). Each contour line represents a 1% decrease in the maximum possible fuel efficiency in that condition. The contour plot is specific to aircraft type, weight, and atmospheric condition. Efficiency improvement potential can be measured by comparing as-flown speeds and altitudes to optimal conditions at every point in a flight.

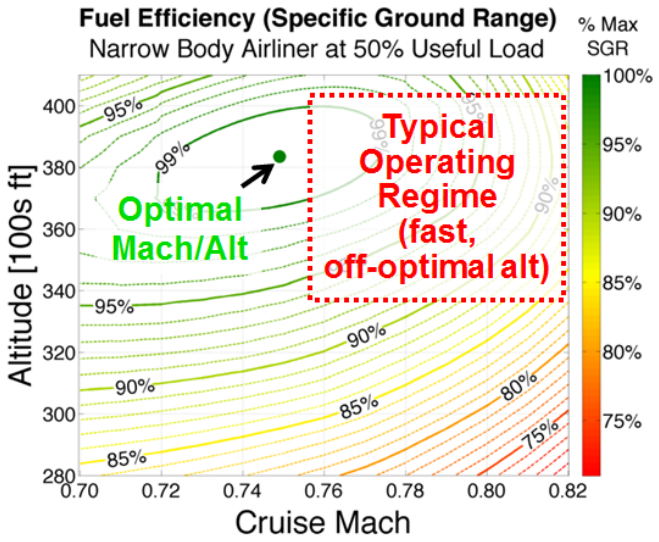

Figure 2. Fuel efficiency variation with speed and altitude at a fixed weight for a typical narrowbody airliner

Lovegren and Hansman examined 257 flights operated on a single day in 2009 and found average cruise-phase fuel burn reduction potentials of 2.4% (speed optimization), 1.5% (altitude optimization), and 3.5% (simultaneous speed and altitude optimization) [8]. These results motivate this follow-on investigation to determine more precisely the expected fuel benefits of CASO across a wide range of days, airlines, aircraft types, and operating conditions.

1.2 Research Objective

The primary objective of this research is to quantify and characterize the aircraft fuel efficiency benefits that are achievable through improved altitudes and speeds in the cruise phase of flight. The physics that define cruise performance are already well understood. Aircraft manufacturers provide detailed performance information with an aircraft upon delivery, including fuel burn dependencies on weight, altitude, and speed. Airline dispatchers are able to calculated expected fuel consumption for a given flight using flight planning software and lookup tables. Pilots have access to expected fuel consumption from the flight plan and fine-tuned projections through the onboard Flight Management Computer (FMC). Based on flight plan information, ATC can access total fuel load (in hours) as well as initial altitude and speed assignments. Despite these shared trajectory planning mechanisms, most flights do not operate at fuel-optimal altitudes and speeds. This study aims to quantify the system-level fuel efficiency impact of current off-optimal cruise operations in the National Airspace System based on actual operational data.

The secondary objective of this research is to identify similarities and differences in cruise efficiency between different types of operations. For example, different outcomes may exist based on airline, aircraft type, origin, destination, stage length, direction of flight, and weather

(among other factors). By identifying subsets of all operations in the NAS with particularly high benefit potential from CASO, it becomes possible to recommend implementation policies that target problem areas.

Ultimately, the purpose of this research is not only to quantify the potential fuel efficiency improvements from CASO, but to help identify opportunities for implementation. The results from this research are intended to provide a strong quantitative basis from which stakeholders in the NAS can develop improved cruise procedures.

1.3 Study Scope

The scope of this study is limited to domestic high-altitude airline operations within the continental United States (CONUS). Analysis was limited to this single realm of operations due to (1) the variability in air traffic rules in overwater and international operations and (2) limited high-resolution flight track data availability for other parts of the world. Some of the conclusions may be applicable to certain international operations, depending on airspace congestion levels and flight planning infrastructure. Future phases of this research will analyze specific oceanic and international operations to identify other high-benefit areas for improved altitudes and speed.

Airline operations are the intended focus of the research. General aviation (GA) and military operators account for less than 5% of total fuel burn in the NAS [7], reducing the systemwide environmental impact of optimization in those sectors. Additionally, cost drivers are different for GA and military operations – increased efficiency is often less important than speed and flexibility. Airlines operate at a much larger scale with business pressures that favor minimized cost over raw performance. Therefore, efficiency studies are naturally well-suited for profit-maximizing airline operators. The largest possible environmental benefit from CASO also occurs in the airline sector.

The results of the study are intended to reflect CASO efficiency benefits given current NAS characteristics such as congestion level, fleet mix, separation standards, and technology levels. No single day of operation or subset of an airline flight schedule is adequate to provide this representation. In order to accurately characterize the aggregate system efficiency, it is necessary to look at a wide spectrum of operations to capture the stochastic nature of system performance. Therefore, this study examines 217,000 airline flights from 19 days in 2012.

1.4 Thesis Outline

This thesis begins with an introduction to fuel efficiency in cruise flight. Chapter 2 provides relevant background for the CASO problem. The choice of Specific Ground Range (SGR) as the metric for this study is described. The aerodynamics of jet aircraft cruise efficiency are

introduced along with the impact of wind on optimal trajectory planning. Current practices for speed and altitude trajectory planning are discussed.

Chapter 3 describes the analysis procedure used to calculate the fuel burn benefits expected from CASO. The discussion includes data requirements and assumptions used in calculating as-flown trajectory fuel burn. The algorithms and heuristics used for developing alternate optimized altitude and speed profiles are also introduced.

Chapter 4 presents the results of the CASO study. Descriptive statistics for the expected benefits of each type of optimal profile are provided, along with a variety of comparisons and decompositions of the full output set to illustrate specific system characteristics.

Chapter 5 offers a discussion of results. This includes the identification of operational drivers for certain behavior seen in the results.

Chapter 6 concludes the thesis, highlighting the key results and implications of the study. This section includes a high-level discussion of potential implementation strategies and future research directions.

Page Intentionally Left Blank

Chapter 2 BACKGROUND

2.1 Altitude Planning and Assignment in Practice

In an ideal system, all air traffic would use optimal altitudes at all times. In practice, aircraft are constrained by flight level availability, accuracy of cockpit wind information, airspace congestion, weather, and turbulence. Altitude management occurs in three phases; (1) planning trajectories before each flight; (2) refining planned trajectories with finalized information before takeoff; and (3) modifying altitude trajectories tactically during flight.

Airline dispatch specialists generate a flight plan several hours before every departure. For domestic flights in the CONUS, the route is selected based on several factors such as prevailing winds, convective weather, turbulence forecasts, FAA preferred routing, and airspace traffic management initiatives. Initial altitude is selected based on anticipated aircraft weight, direction of flight, and prevailing wind. This flight plan is transmitted to the FAA and approved as-is or with modifications. The flight plan is also passed to the pilots (in printed form), and in many modern aircraft, directly to the airplane's FMC using the Aircraft Communications Addressing and Reporting Sytem (ACARS). Pilots may accept a flight plan from dispatch without revision or make alterations as deemed necessary.

At the time a flight plan is generated by dispatchers, several factors impacting altitude selection are uncertain. For example, aircraft departure weight is not known with certainty due to variation in cargo loads, passenger show-up rate, and additional fuel requests from the pilots. Weather and winds can also change prior to departure relative to pre-flight forecasts. Therefore, the second phase of altitude management occurs immediately prior to pushback from the gate when pilots enter finalized weights and updated winds into the FMC. The FMC then calculates any necessary modification to the altitude profile.

The third phase of altitude management occurs once an aircraft departs. Air traffic controllers may assign alternate altitudes in response to traffic conflicts. Pilots request tactical altitude changes for several reasons, including updated wind information, high-altitude convective weather, and poor ride conditions. Therefore, altitude changes are sometimes driven by efficiency, but just as frequently by other factors that increase fuel burn as a byproduct. These decisions are based on pilot reports (PIREPS), updated information from ATC or dispatch, and crew experience [9]. While the motivation for requesting an altitude change is often abundantly clear, the time window over which any off-optimal altitude selection should be sustained is not always as obvious.

High altitude airspace in the CONUS contains specific usable cruise altitudes, or flight levels, at 1000 ft increments. Which of these cruise altitudes is available to a flight depends on the

direction of travel and level of congestion in the system. For aircraft equipped for Reduced Vertical Separation Minima (RVSM), including the majority of airline-operated jet aircraft, this normally constrains climbs and descents to occur in 2000 ft increments, as alternating levels serve opposite flight directions. Therefore, flights cannot normally operate at the absolute fuel-optimal altitude in today's NAS, regardless of congestion or weather. Instead, the nearest eligible altitude must be selected, which may be more than 1000 ft above or below the true optimal altitude. RVSM-eligible altitudes for eastbound and westbound flights are shown in Figure 3.

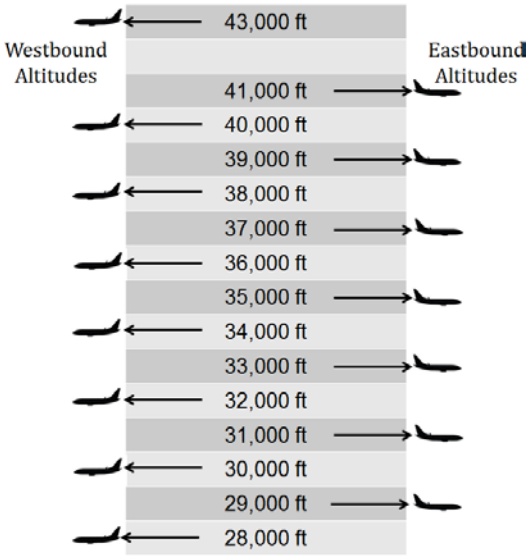

Figure 3. RVSM Eligible Altitudes

Some FMCs provide guidance to pilots about the optimal time to initiate climbs and descents in cruise based on changing aircraft weight and winds. In these systems, the quality of the FMC climb recommendation depends on the accuracy and resolution of wind data. Some airlines have provisions for automatic wind updates through the ACARS system, while others require manual entry by the pilots. In practice, the wind data provided to the FMC is often of low resolution (many systems only accept 3 to 5 wind reference points per trajectory) and out of date, having been obtained from a forecasting model during the flight planning process.

For a typical narrowbody aircraft operating near its optimal altitude, fuel efficiency drops by 1% with a climb or descent of about 1500 ft. As the cruise altitude becomes further from optimal, the response of fuel consumption to altitude becomes more sensitive. Clearly, operations away from optimal altitude profiles can increase systemwide fuel consumption. Significant perturbations from optimal altitude (on the order of 6,000-8,000 feet) can increase fuel burn by over 10%.

2.2 Speed Planning and Assignment in Practice

Speed planning occurs in the same two stages described for altitude planning. Dispatchers provide an initial flight plan with a detailed speed schedule for every flight. Once the flight is airborne, pilots and ATC can alter speeds to satisfy tactical constraints, absorb delay, or respond to changing conditions.

Airline dispatchers generate the initial speed trajectory for a flight using flight planning software and aircraft-specific documentation. The fundamental consideration when selecting speeds is to minimize the cost to the airline network for operating a specific flight. Minimizing cost in cruise involves a tradeoff between time costs and fuel costs. Time costs include items such as crew pay, aircraft depreciation and ownership, and maintenance. If all flights were operated at absolute fuel-optimal speed (MRC) speed, average flight times would increase. However, there exists a faster speed at which the marginal time cost reduction equals the marginal fuel cost increase. By operating at this balance point, total operating costs can be minimized on a single flight and over a full network [10].

Dispatchers use the Cost Index (CI) as a metric for communicating the value of time relative to the value of fuel. CI is most clearly conceptualized as the slope of the fuel efficiency curve as shown in Figure 4. Therefore, the exact speed that corresponds to a particular CI value depends on the shape of the efficiency polar for a particular aircraft, weight, and wind condition. Furthermore, there is no industry-standard unit or scale for CI values, meaning that a specific numeric input will have a different impact on different aircraft types and different FMC models. Typical values range between 0 and 9,999. In all cases, a CI of zero minimizes fuel burn while a CI at the top of the scale results in maximum speed.

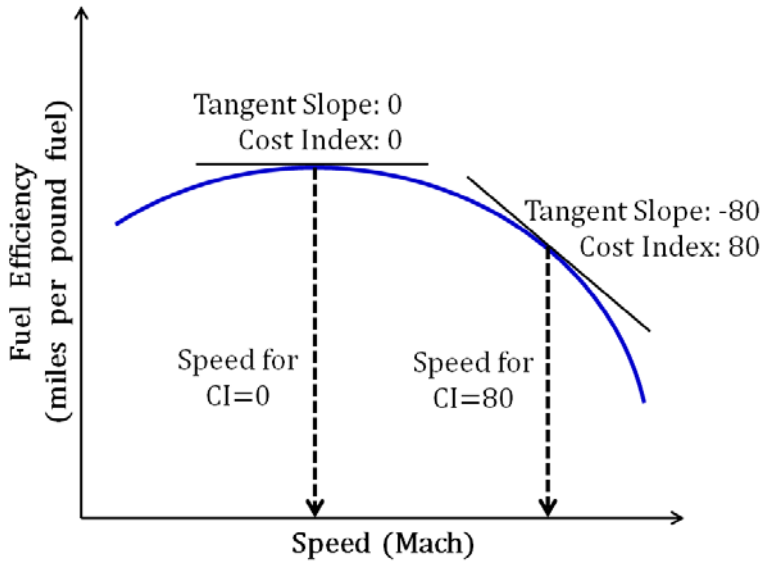

Figure 4. Representation of Cost Index as the derivative of a notional fuel efficiency polar.

The challenge with using CI is determining accurate values for the time-based cost contribution. There are so many factors influencing the cost basis for an airline, many of them productivity-driven, that accurately gauging the contribution of a marginal minute on a single flight leg is a very difficult problem. Given volatile fuel prices, changing network demands, and aircraft-specific efficiency characteristics, a precise implementation of CI requires dynamic calculation for every flight, and potentially at multiple points within every flight [11]. The technological and analytical capacity for such calculations is not present at most airlines, meaning that CI is normally used as a simple speed control proxy. Many airlines periodically adjust CI policies based on financial results, schedule structure, and operating priorities, but the analysis leading to such adjustments varies considerably between airlines.

2.2.1 METHODS FOR CRUISE SPEED CONTROL

In airline operations, speed is controlled using two methods. The first is direct speed control by the pilot using manual throttle input or autothrottle. This allows pilots to maintain specific indicated airspeeds or Mach numbers without reference to corresponding efficiency values. This mode is generally used when ATC provides speed clearances or the aircraft is not equipped with a functional FMC.

The second method for speed control is to use one of the trajectory selection modes in the FMC. There are several speed control options available, including:

1) **Long Range Cruise (LRC)**
   This FMC function provides an automatic calculation of LRC speed at all times during flight. LRC is an industry-standard metric that addresses the tradeoff between time and fuel with a simple percentage-based approach. LRC is defined as the speed faster than the absolute fuel-optimal speed where efficiency has been degraded by 1%. The cruise speed increase for this reduction in cruise efficiency can be as high as 3-5% [12]. This particular time vs. efficiency tradeoff point is used somewhat arbitrarily, but has become an industry standard. LRC speed is one of the optimization outputs generated in this study.

2) **Cost Index (CI) / Economy**
   This FMC function uses a CI provided with the flight plan or directly by the pilots. When a CI value has been entered in the FMC, cost-optimal speeds can be calculated automatically that balance the costs of time and fuel. The CI value is used by the FMC to calculate "Economy" speeds and vertical navigation (VNAV) profiles. CI-based optimization profiles are not generate in this study, although basic time and fuel interactions are explored through the LRC optimization metric.

3) **Required Time of Arrival (RTA)**
   Some new-generation FMC systems support RTA speed control. Rather than assigning speed directly, a time constraint is placed on one of the waypoints in the flight plan. A

speed is calculated and adjust dynamically in order to arrive at the metering fix at the RTA. This is an important part of the 4-D Trajectory Based Optimization (4D-TBO) component of the Next Generation Air Transportation System under development by the FAA [13]. While the FMC function itself does not attempt to maximize fuel efficiency, effective RTA clearance design should be able to incorporate concepts of cruise speed efficiency.

The FMC plays a central role in speed optimization in day-to-day airline operations. The optimal output from the computer depends on accurate input of aircraft weight and weather. Given accurate information, current FMCs are capable of implementing the cruise speed efficiency concepts discussed in this study.

2.2.2 TACTICAL SPEED CONTROL

It is sometimes necessary for flights to alter planned speed profiles enroute. ATC may request pilots to change speed whenever necessary, normally on account of separation or traffic flow management (metering). Pilots may request changed speeds as well, normally on account of schedule constraints or delay recovery. Actual speed changes are normally implemented using the autoflight system and can be input through the FMC (CI and LRC inputs) or as direct speed commands to the autopilot.

Tactical speed control is generally not motivated by efficiency. Pilots and dispatchers may override flight-planned optimal speeds during times of delay recovery, for example. Air traffic controllers may issue speed commands in conjunction with passing maneuvers, holding, and metering – all of which take aircraft off of optimal planned trajectories.

For a typical narrowbody aircraft operating near its optimal speed, fuel efficiency drops by 1% with a speed increase or decrease on the order of Mach 0.03. As the speed becomes further from optimal, the rate of efficiency falloff becomes higher. That is, the aircraft is least sensitive to speed when operating near the optimal condition but increasingly sensitive the further from optimal the trajectory becomes.

2.3 Fuel Efficiency Metric Selection

This study uses Specific Ground Range (SGR) to evaluate absolute fuel efficiency. SGR is analogous to the miles-per-gallon of an automobile, measuring an aircraft's ground range per pound of fuel consumed. SGR is a wind-corrected form of Specific Air Range (SAR), a metric commonly used to measure distance flown through the air per pound of fuel consumed. SAR is an instantaneous measurement, changing with aircraft speed, altitude, weight, power setting, and aerodynamic configuration. SGR varies with the same factors plus wind, as shown in Eq. 1.

$$SGR = SAR \times \frac{GS}{AS} = -\frac{dR}{dW_f} \quad (1)$$

Where GS = Groundspeed
AS = Airspeed
R = Ground distance (given actual winds)
W_f = Fuel weight

Minimizing this value at all points in a flight (accounting for winds and aircraft weight) minimizes the total fuel consumption. Integrating SGR across the full cruise trajectory yields total cruise fuel burn.

SGR is an appropriate metric for this analysis because it identifies off-optimal operations on a flight-by-flight basis. This allows for analysis on a regional level (subsections of full cruise trajectories) as well as on a flight level. While SGR does not allow calculation of normalized fuel inefficiencies by useful output (i.e. number of passengers), if such information was desired for ranking or policy reasons the flight-level output could be processed further.

2.4 Aircraft Performance for Fuel-Optimal Cruise

An airliner in cruise flight operates in a state of level, unaccelerated flight. In this condition, the lift force exactly counteracts the aircraft's weight while engine thrust exactly counteracts the drag force. Figure 5 shows the relationship of these force vectors on an aircraft in cruise flight. The lift generated by a wing is a function of the geometry of the wing, angle of attack (AOA), free-stream velocity (or True Airspeed), and air density. The AOA is the angle between the extended wing chord and the relative wind. In order for a wing to generate lift, the AOA must be positive.

It is well-known that the cruise condition for maximum fuel efficiency in a jet aircraft occurs at a specific angle of attack (AOA) [14]. The derivation of this angle of attack involves the fuel flow and thrust characteristics of a jet engine as well as the aerodynamics of the aircraft and occurs roughly where the aircraft velocity per unit thrust is maximized. For most airliners, this cruise-optimal AOA is between 1 and 3 degrees. In order for the aircraft to maintain level flight at this AOA, the combination of true airspeed and air density must result in the correct lift to exactly counteract the weight of the aircraft. If the combination of optimal AOA, density, and velocity results in lift that exceeds weight, the aircraft will climb. If weight exceeds lift, the aircraft will descend.

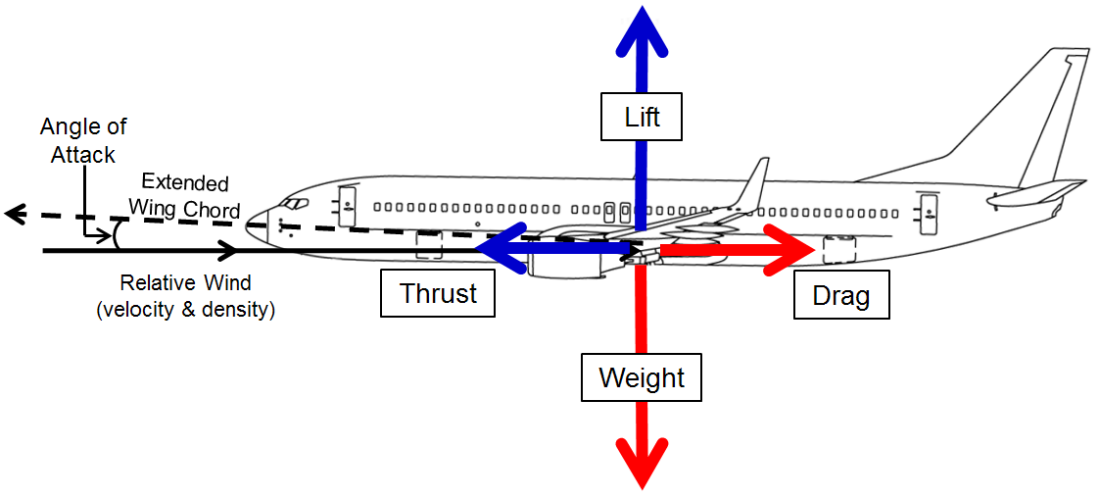

Figure 5. Forces acting on an aircraft in level unaccelerated flight

These observations have direct implications for an aircraft's optimal speed and altitude in cruise. Fuel efficiency involves a combination of aerodynamics and engine performance. Jet engine efficiency tends to increase with altitude, reaching a maximum efficiency within a certain range of fan rotation speeds. To the first order, an optimal fuel condition exists when the engines operate at the most power-efficiency setting, the AOA is at its maximum-range value, and the resulting true airspeed and density result in lift exactly equaling the aircraft's weight.

Altitude plays a central role in this relationship because density decreases with altitude. Therefore, lift generation is lower as altitude increases at fixed true airspeed. If the optimal AOA generates excess lift at a particular altitude and speed, level flight can be restored by reducing AOA to a sub-optimal level, reducing speed, or climbing. There exists an optimal combination of altitude and speed that balances the requirements for optimal cruise condition and engine efficiency.

In this study, adjustments to speed and altitude are shown to have an impact on total fuel burn. This is because, physically, these adjustments alter the AOA required to maintain level unaccelerated flight. The object of CASO is to ensure that the cruise phase is carried out as closely as possible to the optimal AOA.

Page Intentionally Left Blank

Chapter 3 METHODOLOGY

3.1 High-Level Approach

In order to determine the fuel efficiency benefits of CASO on a large number of historical flights, an analysis method was developed that consists of a flight-by-flight examination of radar tracks and weather data from actual days of operation. Each flight is first analyzed as-flown and with several speed and altitude trajectory modifications applied. The fuel burn estimates from the optimal trajectories are compared to the as-flown baseline to determine total benefits from CASO. Figure 6 shows a functional summary of the analysis methodology. This is a refinement of an analysis framework developed by Lovegren in 2012 with extended optimization and post-processing capabilities [8]. Each component of the process is described in detail in following sections.

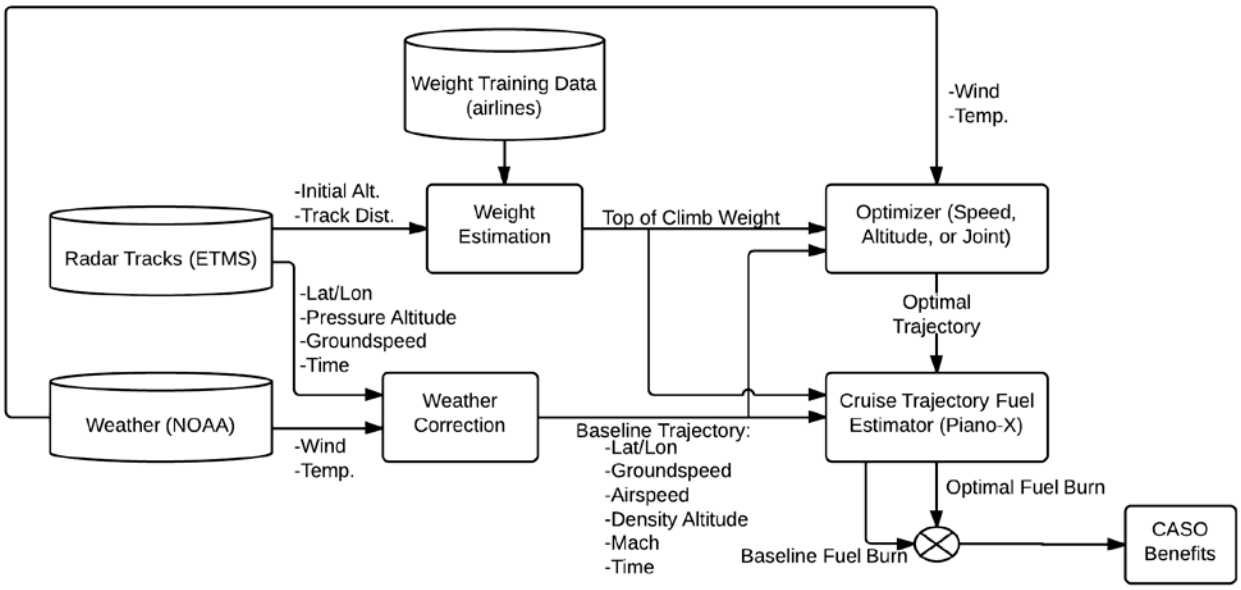

Figure 6. Functional flowchart for the CASO baseline trajectory fuel analysis

The remainder of this section discusses the purpose and functionality for each part of the analysis. The chapter is structured to mirror the process shown in Figure 6.

The analysis begins with raw data for radar tracks and weather. Data sources for these two key inputs are discussed in Section 3.2. In order to condition the input data for the cruise trajectory fuel estimator, it is necessary to remove noise and artifacts from the radar track records. This process is described in Section 3.2.3.

Next, the sample set of flights is selected. The days on which flights occur are required to meet certain case-day criteria, while flights within each sample day have several further criteria for inclusion in the analysis. The sample set definition process is described in Section 3.3.

In order to convert the radar's ground-reference speed data to air-referenced Mach, a weather correction procedure is applied. Pressure altitude is also converted to density altitude, a key variable in aircraft performance. The result of this initial process is a fully-defined baseline trajectory consisting of airspeeds, groundspeeds, Mach numbers, waypoints, and crossing times for every interval of the cruise phase at the same resolution at which the radar data is provided. The weather correction procedure is described in Section 3.4.

In parallel to this computation, aircraft weight is estimated using a surface regression trained with sample data provided by several airlines. Weight is a key driver of aircraft fuel burn and performance, but is not available in any publicly available dataset. This weight estimation routine is described in Section 3.5.

With a fully-defined trajectory and a weight estimation established, the cruise trajectory fuel estimation routine can be implemented. This process loops over every segment of the cruise phase, calculating fuel burn at each stage and updating weight. The difference between input and output weight yields the fuel burn estimate for a trajectory. This process is described in Section 3.6.

Cruise trajectory optimization was implemented in several different ways depending on the desired output. The altitude trajectory optimizer described in Section 3.7 requires a preliminary run of the fuel burn estimator followed by a trajectory fitting or graph search procedure. The speed trajectory optimizers described in Section 3.8 use a looping structure on the baseline trajectory and outputs the optimized trajectory directly. The joint speed and altitude optimizer described in Section 3.9 is schematically similar to the altitude optimizer, requiring a preliminary fuel burn estimation run followed by a graph search routine to identify the final optimal trajectory. In all cases, the optimized trajectory is sent to the same cruise trajectory fuel estimation routine described in Section 3.6.

In order to determine system trends based on the results from many individual tracks, a results database is constructed that records CASO benefits, trajectory definitions, and track identifying information. This database is used for output analysis.

3.2 Data Sources

This analysis is scoped for domestic operations within the CONUS. For each flight, the method requires input data for:

- Historical weather, including wind vectors and temperatures at altitudes of interest
- Flight path, including latitude/longitude traces, altitudes, and timestamps

3.2.1 WEATHER DATA

The purpose of weather data in this study is to convert groundspeed to airspeed (using wind records), airspeed to Mach number (using temperature records), and pressure altitude to density altitude (using temperature records). These corrections are necessary because Mach number and density altitude determine aircraft performance in cruise, not the ground-referenced data observable by surface surveillance. Therefore, the most important characteristic for the weather product used in this analysis is accuracy relative to conditions that actually existed.

Weather data is obtained from the National Oceanographic and Atmospheric Administration (NOAA) North American Regional Reanalysis (NARR). This product synthesizes weather observation data from multiple sources to provide a comprehensive record of actual conditions on the surface and aloft. The data sources used to assimilate wind fields in NARR include radio-tracked weather balloons and aircraft-deployed sensors (radiosondes and dropsondes), visually-tracked pilot balloons, direct measurements from aircraft, and cloud drift from geostationary satellite imagery [15]. NARR is not a forecast product available to flight planners or traffic managers, but a truth product recording conditions that existed based on the best-available information after the fact. As such, NARR would not be available for pre-flight trajectory planning, but is appropriate for post-flight analysis. Figure 7 shows sample NARR output for winds aloft.

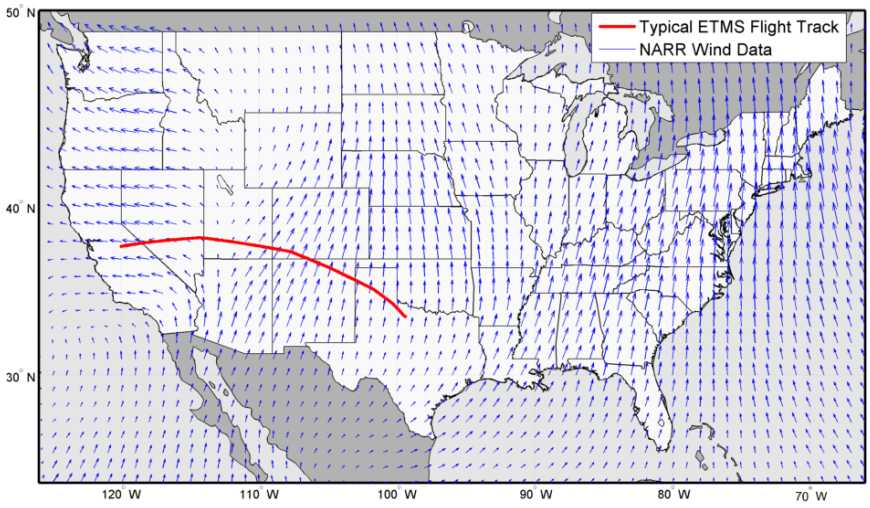

Figure 7. NARR wind data for 34,000 ft overlaid on a sample ETMS flight track

NARR data spans all North American airspace on a 32km lateral grid. In the vertical dimension, the grid includes 29 pressure levels spanning from Sea Level to 53,000 ft in a standard atmosphere. Eight of the available pressure levels span the normal cruise altitudes for commercial airlines, listed in Table 1. Data is provided in 3-hour intervals. For the purpose of this study, weather conditions encountered by a flight at a specific time, location, and pressure altitude are calculated by interpolating NARR records both spatially and temporally.

Table 1. Pressure levels available in NARR for interpolation at normal commercial airliner cruise altitudes

Pressure Level (mb)	Standard Atmosphere Altitude (nearest 100 ft)
350	26,600
300	30,100
275	32,000
250	34,000
225	36,200
200	38,700
175	41,400
150	44,700

3.2.2 RADAR DATA

Radar data is obtained from the FAA's Enhanced Traffic Management System (ETMS). ETMS stations display and log fused flight track records from the full network of domestic Airport Surveillance Radars (ASRs). Traffic managers use the system as a real-time monitor of ATC system performance. Logged ETMS records provide historical flight trajectory data for flights inside North American airspace operating under instrument flight rules. This includes domestic US airline operations as well as many general aviation flights, for a total flight record on the order of 50,000 operations per day. ETMS trajectory information is logged at 60-second intervals, nominally covering all flight phases inside the coverage area from initial climb to final descent. ETMS data fields include airline, flight number, aircraft type, latitude, longitude, altitude, groundspeed, and time.

3.2.3 PRE-PROCESSING TRAJECTORY DATA

ETMS flight trajectories must be processed for data irregularity, incompleteness, and smoothness before cruise efficiency analysis can be undertaken. Because the sample set consists of 217,000 flights, these steps must be completed algorithmically. The first step is to remove altitude data artifacts from the ETMS records. These artifacts are characterized by an instantaneous and short-term change in altitude from the cruise altitude to sea level, as illustrated in Figure 9. Filtering is accomplished using the Despeckle filter proposed by Palacios and Hansman [16].

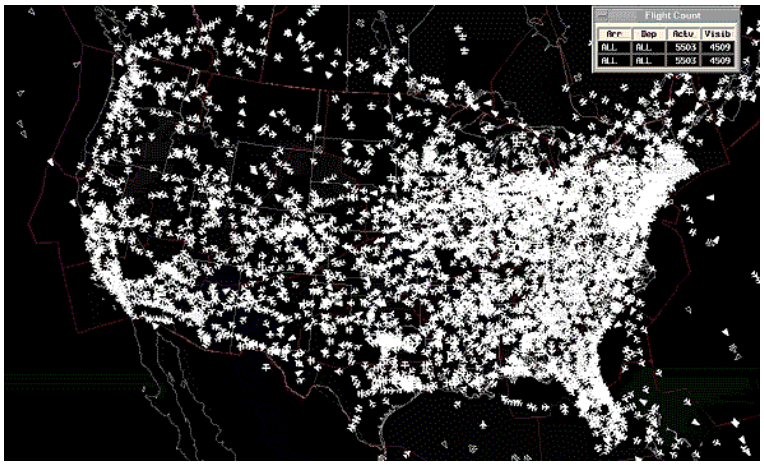

Figure 8. ETMS system status display like those available to ATC facilities (Source: NASA)

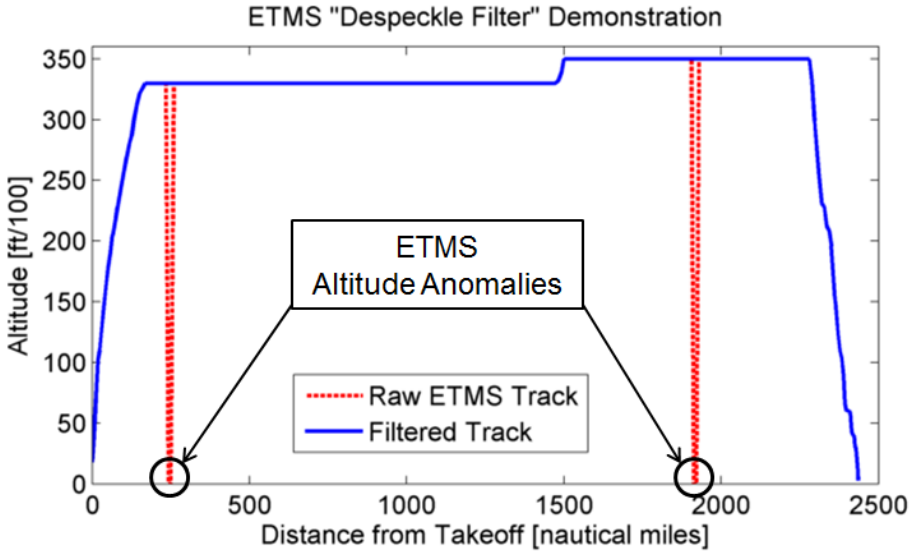

Figure 9. Illustration of ETMS altitude artifacts and corrections

The next requirement is to identify the cruise segment of each trajectory. For the purpose of this analysis, a cruise segment is defined as any period of level flight lasting 10 minutes or longer above 28,000ft. The full cruise phase is the joint set of all such contiguous segments, including climbs and descents that occur within cruise to connect successive periods of level flight. An example of a full cruise phased based on this definition is shown in Figure 10. Fuel efficiency analysis and optimization is performed on the identified cruise phase of each flight. Any flight with no identifiable cruise segment is omitted from further analysis.

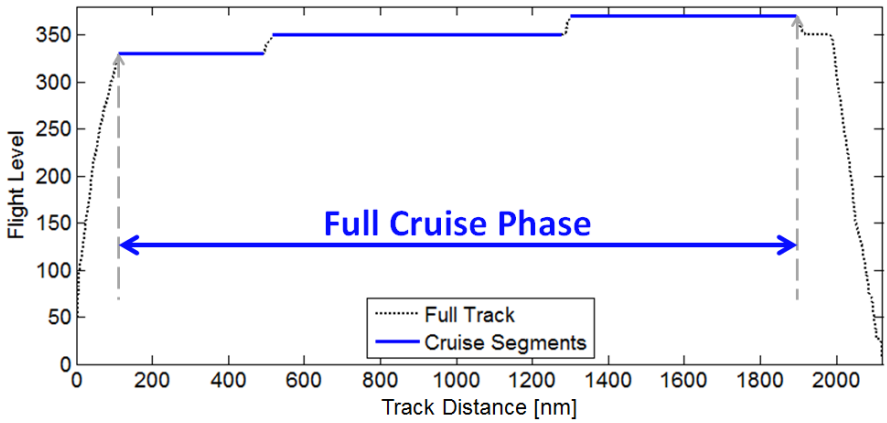

Figure 10. Illustration of cruise segment selection from full ETMS altitude track

Finally, the groundspeed records for the cruise phase of flight are smoothed using a moving average filter to reduce noise in ETMS-reported values. This noise, illustrated in Figure 11, does not reflect actual fluctuations in cruise speed. Aircraft in cruise flight do not normally change speed appreciably from minute to minute. Smoothing the groundspeed tracks reduces high-frequency fluctuations in calculated fuel consumption. Figure 11 illustrates the noise present in ETMS speed records and the smoothing applied prior to CASO analysis.

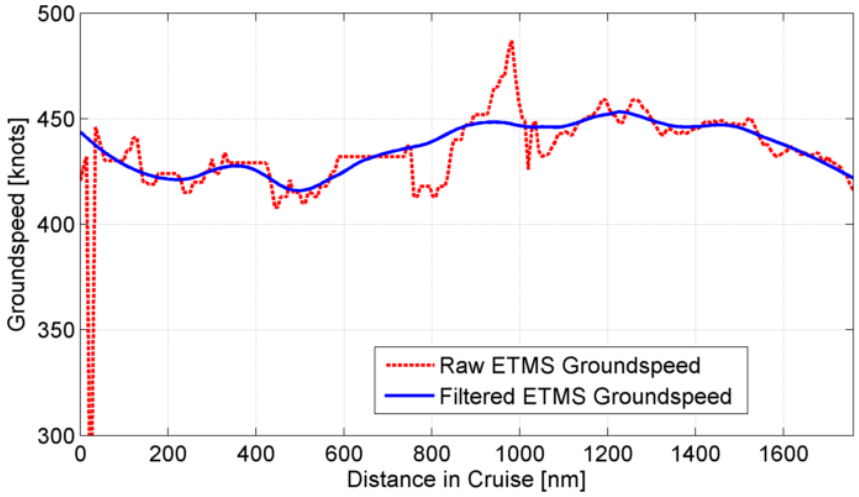

Figure 11. Example of ETMS groundspeed smoothing

3.3 Sample Set Definition

Due to an automated analysis methodology, the sample set for this study could be made much larger than in prior studies with similar objectives. The set consists of 217,000 flights spanning a variety of airlines, routes, aircraft types, and system states.

3.3.1 SELECTING CASE DAYS

Multiple case days were needed in order to capture differences in altitude and speed optimality both with and without airspace congestion. Congestion has two potential effects. First, desired speeds and altitudes are less likely to be available for all flights due to ATC spacing requirements. This impacts both speed and altitude efficiency. Second, the total number of delayed flights is likely to be higher on days with congestion. Confronted with many flights operating behind schedule, airline prioritization of efficiency vs. timeliness can change. This impacts speed efficiency more than altitude efficiency. Without examining data from both congested and uncongested days, this variety in behavior would not be captured.

The days for which flights were analyzed were chosen based on the systemwide state of weather, delays, and flow control programs. The flight track dataset used in this analysis spanned 19 days throughout calendar year 2012, representing a variety of nominal and off-nominal system congestion states. The FAA Aviation System Performance Metrics (ASPM) database was used to evaluate candidate days based on the total number of arrivals impacted by Ground Delay Programs (GDPs), a specific type of traffic management initiative (TMI). Additionally, a daily list of advisories and delay programs issued by the FAA's Air Traffic Control System Command Center (ATCSCC) was cross-checked to determine the extent and severity of NAS disruptions.

For the purposes of this research, nominal days were characterized by minimal service disruption and delays throughout the NAS. Traffic at several key airports correspond to the smooth operation of the NAS as a whole, so the evaluation of candidate days focused on these airports: JFK, LGA, EWR, ORD, IAD, BOS, and ATL. The chosen nominal case days were 2/9/2012 and 6/28/2012, both of which exhibited benign weather with very few delay programs imposed by the ATCSCC.

Off-nominal days were characterized by traffic flow disruptions over large areas of the NAS. The purpose of analyzing off-nominal NAS scenarios was to compare fuel efficiency against the nominal baseline for operations arriving or departing from specific impacted airports. Efficiency cannot be determined for cancelled flights, so off-nominal case days were chosen to have widespread TMIs without accompanying cancelations. Off-nominal days were selected for each of 7 geographic regions, representing a wide variety of weather conditions and delay scenarios. The case days shown in Table 2 were selected based on ASPM data at major airports in each region.

Figure 12 shows an example of the ASPM and weather metrics used to classify nominal- and off-nominal sample days in this study. The figure corresponds to May 21, 2012, selected as an off-nominal sample day for the Northeast region. The number of flights assigned Expected Departure Clearance Times (EDCTs) indicate the level of TMI intervention at several important airports within this region. Weather radar indicates widespread convective activity throughout the eastern states, likely the cause of the GDPs. NAS performance overview records also show an

abnormally large number of program advisories for the day, confirming it as a good off-nominal case day. The other case days were evaluated in a similar manner.

Table 2. Sample days with localized (regional) congestion and/or weather

Region	(Representative Airports)	Case Days (2012)
Northeast	(JFK/EWR/BOS/DCA/PHL)	5/21 and 12/10
Southeast	(ATL/CLT/DCA/MEM)	1/23 and 2/24
Midwest	(ORD/MDW/DTW/STL/MSP/MCI)	4/20, 5/1, and 5/30
Northwest	(SFO/SEA)	1/30 and 5/17
Southwest	(LAX/SAN/PHX/LAS)	7/22, 8/22 and 12/13
Rockies	(DEN/SLC/ABQ)	2/3, 4/6, 10/16
Texas/Gulf Coast	(DFW/IAH/HOU)	1/22 and 7/7
Nominal	Unconstrained Throughout NAS	2/9 and 6/28

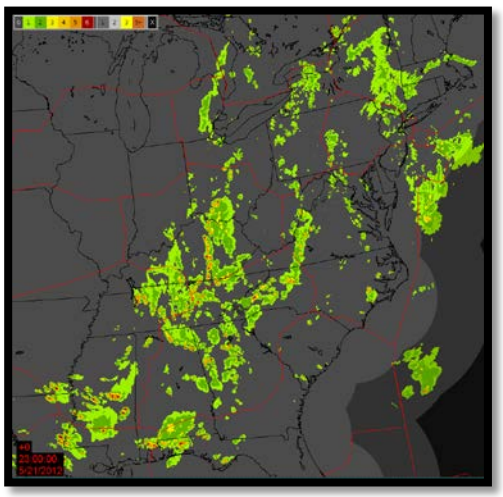

EDCT Report

From 5/21/2012 To 5/21/2012 : 'ATL,BOS,EWR,IAD,JFK,LGA,ORD'

Scheduled Departure Date	Airport	Arrivals For Metric Computation	Arrivals With EDCT	% Of Arrivals With EDCT	Avg EDCT For All Arrivals
05/21/2012	ATL	1329	333	25.06	9.73
05/21/2012	BOS	475	157	33.05	11.25
05/21/2012	EWR	548	333	60.77	31.08
05/21/2012	IAD	422	0	0	0.00
05/21/2012	JFK	528	140	26.52	5.62
05/21/2012	LGA	540	406	75.19	33.91
05/21/2012	ORD	1254	0	0	0.00

Figure 12. Sample evaluation metrics used to classify and prioritize case days: weather reports (left) and GDP records (right)

3.3.2 Selecting Flights Within Case Days

All eligible flights within the ETMS database for each case day were included in the analysis sample set. Eligibility criteria included (1) flight departure and arrival within the CONUS; (2) aircraft type inclusion in the set of 44 eligible Piano-X aircraft models; (3) minimum 10-minute identifiable cruise segment above 28,000 ft; (4) identifiable climb and descent phase in the ETMS record to ensure that the full cruise phase is represented. Of all flights in the daily ETMS record, about 34% meet each of criteria (1)-(4). This results in a sample size ranging from 10,000-13,000 flights per sample day.

3.4 Weather Correction

For each data point in the ETMS radar track record, groundspeed and pressure altitude must be converted to Mach number and density altitude. This is because the Piano-X point performance calculator outputs air-referenced efficiency (SAR) based on air-referenced performance criteria. The process by which ETMS data is converted to Mach and density altitude is summarized in Figure 13.

For each point in the radar track, the corresponding wind and temperature are extracted from the NARR database. These variables are then applied to the radar track information. First, wind data is used to convert groundspeed to true airspeed using vector addition. Groundspeed determines flight time between two points, but airspeed determines aircraft performance.

Second, airspeed is converted to Mach number. Mach number is the ratio of true airspeed to the local speed of sound. Aircraft performance depends strongly on Mach number in high-altitude cruise flight. Temperature data is used to convert airspeed to Mach number based on the following relationship:

$$M = \frac{v}{c} = \frac{v}{\sqrt{\frac{\gamma RT}{M_{air}}}} = \frac{v}{\sqrt{401.882T}} \text{ for dry air} \quad (2)$$

Where M = Mach number
v= True Airspeed (meters per second)
c= Speed of Sound (in dry air)
γ = Heat Capacity Ratio (1.4 for ideal, dry air)
R = Molar gas constant (8.3145 J $*$ mol^{-1} $*$ K^{-1} for ideal, dry air)
T = Atmospheric Temperature (Kelvin)
M_{air} = Molar Mass of Air (0.02896 kg $*$ mol^{-1} for ideal, dry air)

Third, pressure altitude is converted to Density altitude. Aircraft flight instruments determine altitude based on the atmospheric pressure, not density. Atmospheric density also has a large impact on aircraft performance. Density altitude corrects pressure altitude for non-standard temperature. When temperature is warmer (colder) than standard, density altitude is higher (lower) than pressure altitude. Density altitude determines aircraft and engine performance. Air density is calculated using a standard atmosphere temperature offset lookup table. The altitude in a standard atmosphere corresponding to this density is then returned as the density altitude.

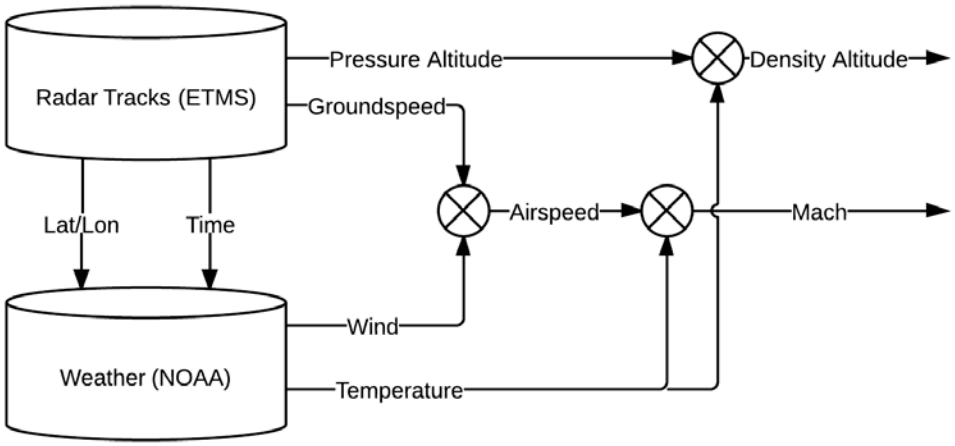

Figure 13. Process for converting ground-reference ETMS data to air-reference data using weather model

Together, these three conversions condition the trajectory data for input to the aircraft performance model, since it is Mach and density altitude that determine fuel burn in the high-speed cruise regime.

Optimal cruise conditions are strongly affected by atmospheric conditions. In general, optimal speed increases in a headwind and decreases in a tailwind. This minimizes the overall time exposure to headwinds and maximizes the time exposure to tailwinds. Winds that change with altitude can also drive optimal speeds and altitudes to drastically different values compared to the calm-wind scenario. Figure 14 shows the impact four hypothetical wind gradients on SGR in an otherwise-standard atmosphere.

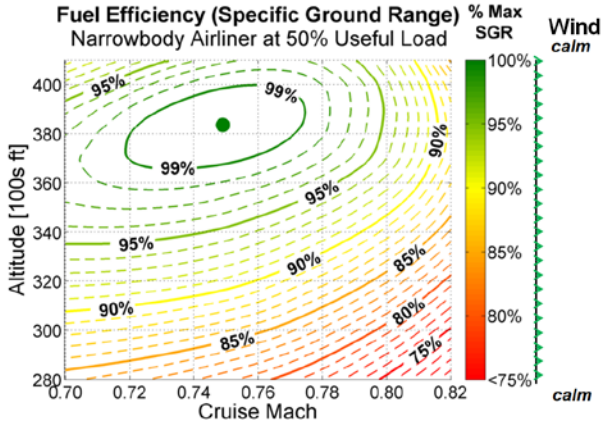

(a) Calm Wind

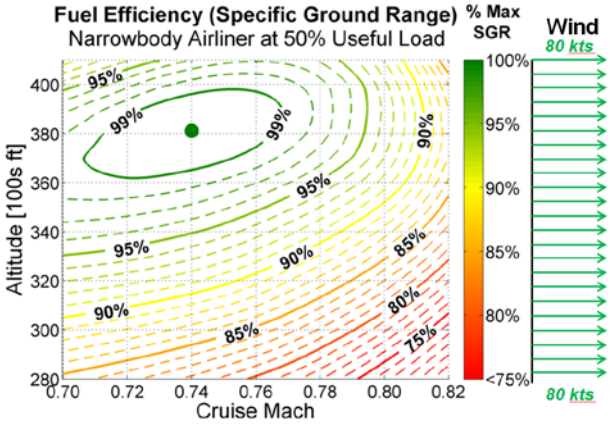

(b) 80-knot tailwind at all altitudes

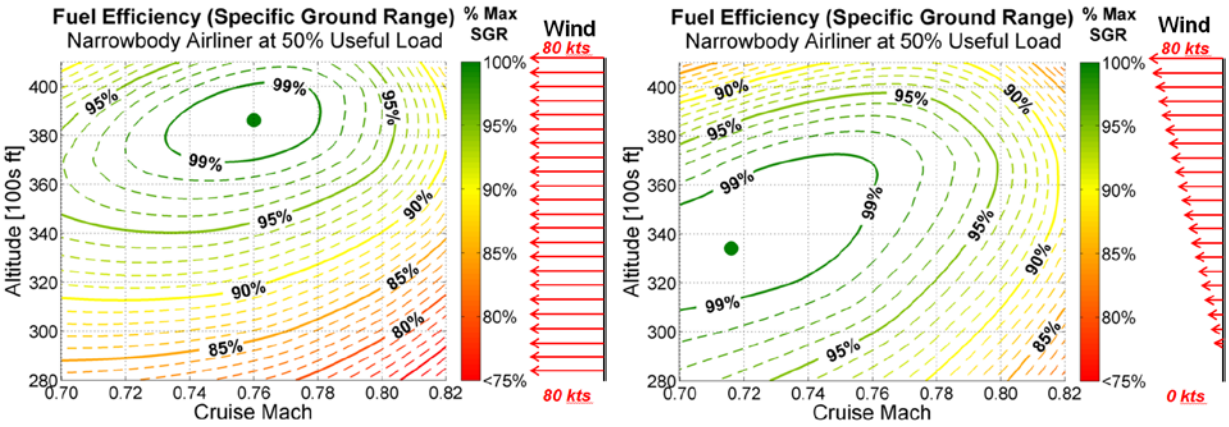

(c) 80-knot headwind at all altitudes

(d) Calm wind at low altitude growing to 80-knot headwind at high altitude

Figure 14. SGR efficiency contours for a typical narrowbody aircraft at fixed weight in different wind conditions

In Figure 14, subfigure (a) shows the no-wind SGR, equivalent to the aircraft's SAR at the given weight. Subfigure (b) shows the reduction of optimal cruise speed by Mach 0.01 in the presence of an 80-knot tailwind, along with a 200 ft decrease in optimal altitude. This altitude change occurs because reducing speed moves the aircraft away from optimal cruise AOA. This is counteracted by descending to denser air at lower altitudes, allowing the aircraft to operate at an optimal angle of attack despite the new lower airspeed (described in Section 2.4). Subfigure (c) shows an increase in optimal speed in the presence of an 80-knot headwind, along with an increase in optimal altitude of 200 ft. This altitude adjustment occurs for similar reasons to the tailwind case.

Subfigure (d) shows the major impacts of wind speed gradients on optimal altitude planning. In this case, a strong headwind at the normal optimal operating altitude drives the optimal point to a lower flight level experiencing less wind. Such wind speed gradients exist in the actual atmosphere, such as near jetstream shear layers and frontal boundaries underneath the tropopause.

3.5 Weight Estimation

Weight is one of the most important factors affecting the fuel burn model in this study. Figure 15 shows the relationship between optimum cruise Mach and aircraft weight for a typical medium range airliner. Absolute fuel efficiency increases with decreasing weight because less thrust is required to produce sufficient lift for level flight. The optimal speed also changes with weight, becoming slower as the aircraft becomes lighter. A similar relationship exists between

optimal altitude and weight as shown in Figure 16. The optimal altitude increases as the aircraft becomes lighter.

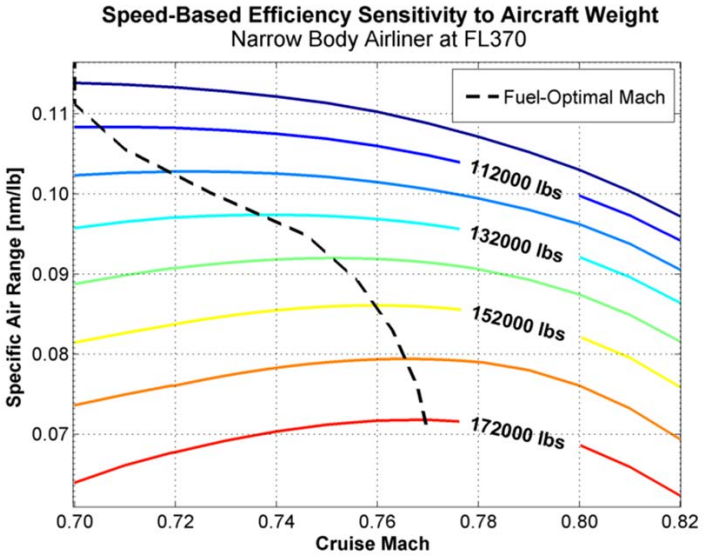

Figure 15. Optimal calm-wind cruise Mach at various weights for a typical narrowbody aircraft assuming constant altitude

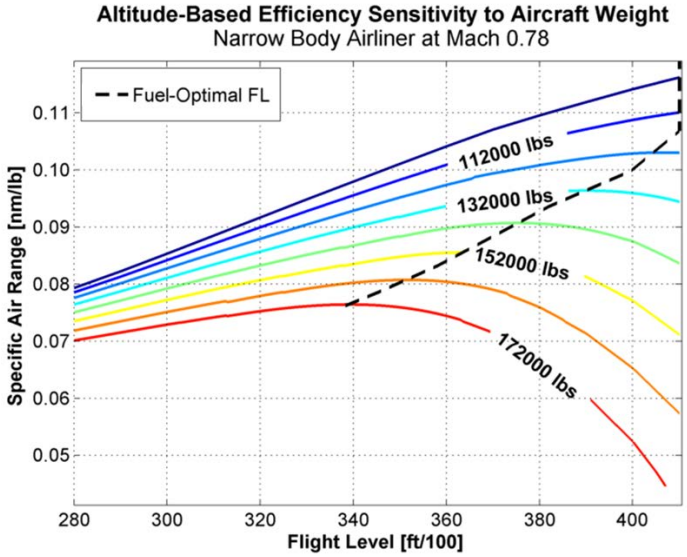

Figure 16. Optimal calm-wind cruise altitude at various weights for a typical narrowbody aircraft assuming constant Mach number

It is clear that aircraft weight directly impacts the optimal altitude and speed in cruise flight. However, no publicly available dataset reports aircraft weight. In order to calculate fuel

consumption, is necessary to estimate weight as accurately as possible on a flight-by-flight basis. This initial weight estimation is an input to the cruise trajectory fuel burn estimator.

For this study, three airlines provided sample takeoff weight (TOW) data from a selection of flights in 2012. This dataset includes weight records for a total of 35,131 individual flights. Each of the carriers serves the domestic US market using a range of narrowbody and widebody aircraft types. This TOW dataset, along with corresponding records from ETMS, allow for an examination of correlations between various flight metrics and initial cruise weight. The objective of the weight estimation function is to estimate top-of-climb weight (TOCW). To convert TOW to TOCW, fuel consumption in climb must be estimated. Piano-X was used to estimate climb fuel as a function of takeoff weight and initial cruise altitude. This estimate was based on an optimal-profile maximum performance climb trajectory given a 250kt speed restriction below 10,000ft MSL (mean sea level).

Statistical analyses determined which variables in the ETMS track record had the strongest correlation to the TOCW. The two best choices include initial cruise altitude and total flight time. These variables were fit simultaneously using a second-order multivariate regression as shown in Figure 17. The figure shows as black circles the data points provided by three airlines for the Airbus A320 representing multiple days in 2012 (9,779 total flights). The resulting weight estimation surface regressed from these data points is shown as well.

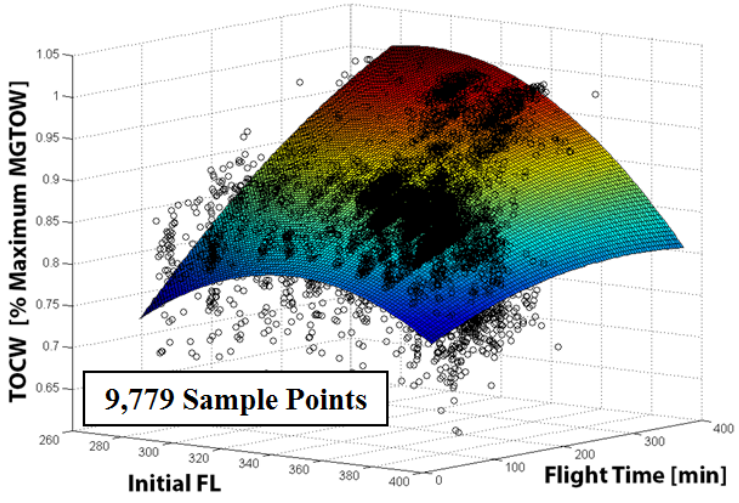

Figure 17. Polynomial least-squares multivariate regression for TOCW as a function of flight time and initial cruise altitude for the Airbus A320

A similar regression was performed for 10 aircraft types with sufficient sample weight data to generate a regression surface. These regression surfaces were used directly to estimate weights for corresponding aircraft types in the full analysis set. For aircraft types not included in

the set of regression surfaces, a generalized regression surface was used that estimated TOCW as a function of the aircraft's Maximum Gross Takeoff Weight (MGTOW) and flight duration. Figure 18 shows the error distribution in weight estimation for the Airbus A320 (based on 9,779 total sample flights). The distribution represents the difference between the training data set and the weight estimation regression model developed using that data.

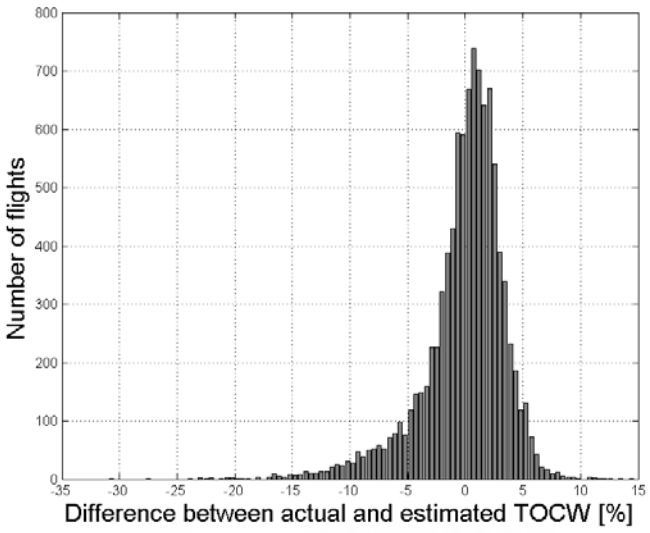

Figure 18. Error distribution of estimated vs. actual weights for the Airbus A320

3.6 Cruise Trajectory Fuel Estimation

This section describes how the point-performance calculator from Piano-X is used to determine full-trajectory fuel burn. Fuel burn is calculated sequentially for each one-minute interval of a cruise phase data. The geographic midpoint of each interval is the reference point at which instantaneous SGR is calculated. The fuel burn along each interval is the instantaneous SGR multiplied by the ground distance of that interval. As the aircraft proceeds along the trajectory, the instantaneous weight is updated to reflect fuel burned in prior segments of cruise. Therefore, the fuel burn estimation model consists of a discretized, sequential aircraft performance lookup procedure using actual track data and weather as input. The output is a detailed weight history at the same time resolution as the input track data (60 seconds for ETMS data).

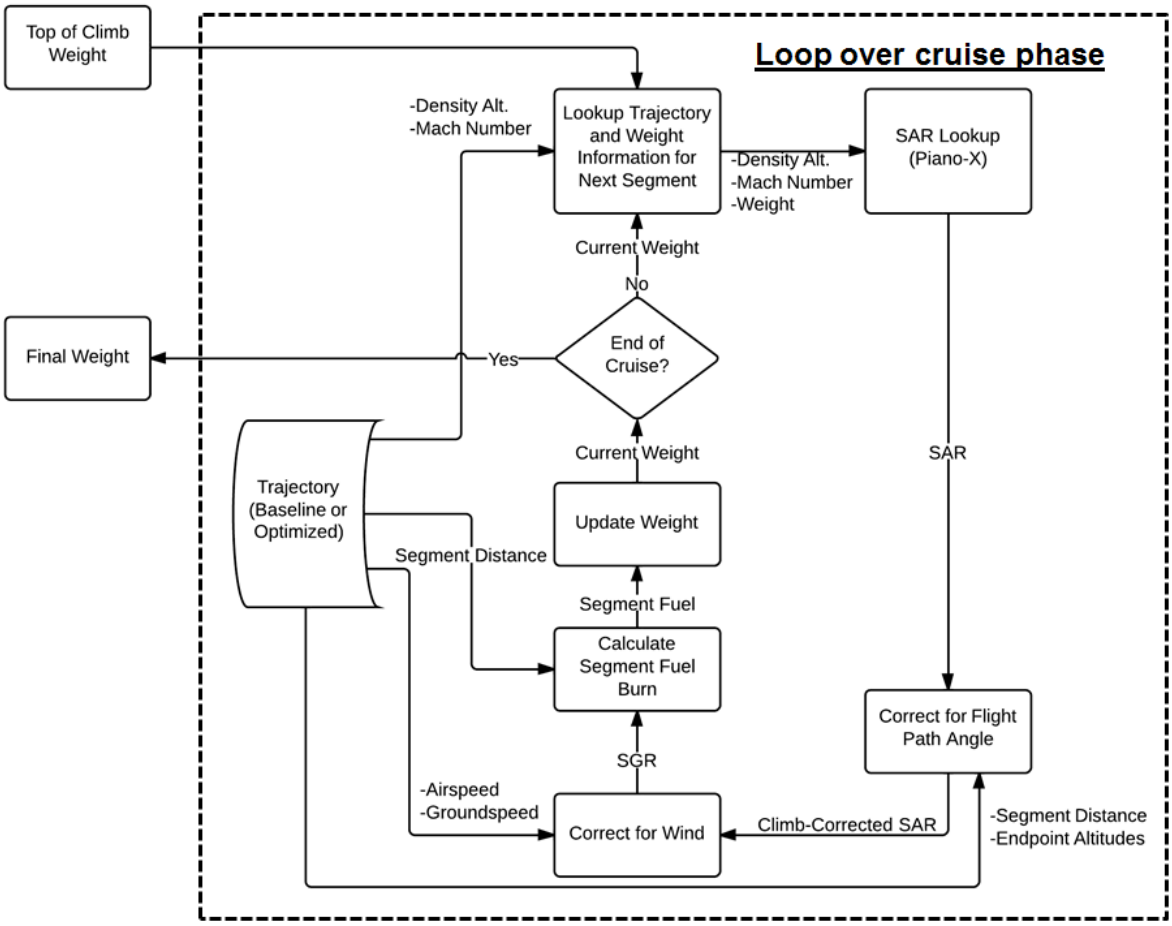

Figure 19. Functional flow diagram of looping structure used to calculate cruise trajectory fuel consumption given a fully-defined trajectory and initial weight

3.6.1 AIRCRAFT PERFORMANCE MODEL

Aircraft performance is modeled using Lissys Piano-X, a commercially-available software package. Piano-X includes a database of over 400 commercial aircraft types, including sub-variants for many common airliners. The performance database is derived from a variety of public and proprietary data sources.

The specific capability of Piano-X used in this analysis is the point-performance cruise calculator. Figure 20 shows the graphic user interface for Piano-X. Given an input state vector of speed, altitude, and weight, the model outputs a clean-configuration steady state performance vector including aerodynamic coefficients, performance margins, and emission metrics. This output vector includes SAR, which can be used in conjunction with wind data to calculate SGR and ultimately full-trajectory fuel consumption. For input state vectors outside the feasible performance envelope for an aircraft (i.e. too fast, too high, or too heavy) the model outputs a

warning flag. This capability prevents the trajectory optimizer from suggesting altitude and speed combinations that cannot be achieved by the aircraft.

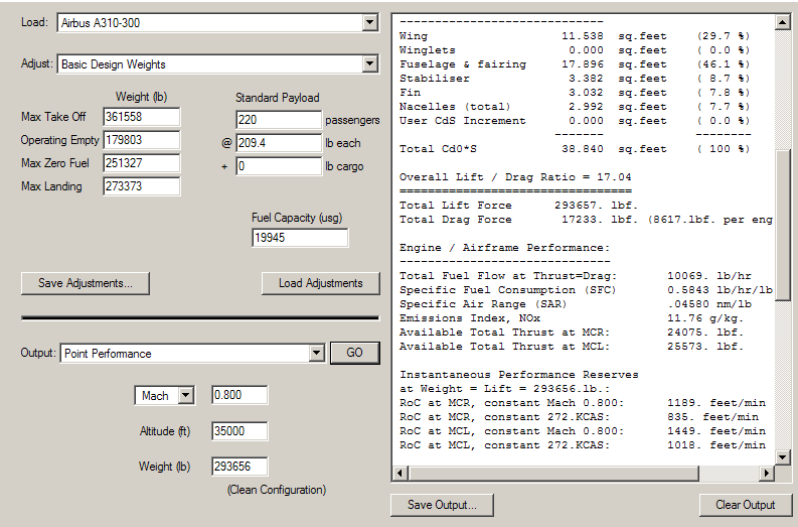

Figure 20. Piano-X point performance calculator user interface

44 aircraft types from Piano-X were included in the analysis, representing 90.1% coverage of all flights recorded in the ETMS database above 28,000 feet. The majority of flights not covered by these 44 aircraft types are GA flights. The full list of the aircraft types included in this study is provided in Table 3.

Aircraft type information available from flight plan records provides the variant (e.g. A320-200, B737-900) without providing details about specific subvariant (e.g. B737-900ER vs. B737-900 with winglets), aircraft age, engine type, or other airframe-specific characteristics. Therefore, the Piano-X model uses a single performance model for all flights operated by the same variant, regardless of which specific subvariant actually operated the flight. This results in some errors in absolute fuel consumption estimation. For example, a flight operated by a winglet-equipped aircraft will burn less fuel than an equivalent flight on a non-winglet aircraft. However, such variation is unavoidable in analysis and the incremental impact of altitude and speed optimization remains similar between subvariants.

Table 3. Aircraft Types Covered in Study

Aircraft Type	Frequency Share*	Aircraft Type	Frequency Share
Airbus A300-600	1.0%	Boeing 767-400	<1.0%
Airbus A310	<1.0%	Boeing 777-200	<1.0%
Airbus A318	<1.0%	Boeing 777-200LR	<1.0%
Airbus A319	5.4%	Boeing 777-300	<1.0%
Airbus A320	7.4%	Bombardier CRJ-100	<1.0%
Airbus A321	1.2%	Bombardier CRJ-200	6.8%
Airbus A330-200	<1.0%	Bombardier CRJ-700	5.6%
Airbus A330-300	<1.0%	Bombardier CRJ-900	2.6%
Boeing 717-200	2.6%	Douglas DC-10	<1.0%
Boeing 727-200	<1.0%	Douglas DC-9-10	<1.0%
Boeing 737-200	<1.0%	Douglas DC-9-30	<1.0%
Boeing 737-300	3.9%	Embraer E-170	3.5%
Boeing 737-400	1.1%	Embraer E-190	1.5%
Boeing 737-500	<1.0%	Embraer EMB-135	1.5%
Boeing 737-700	12.1%	Embraer EMB-145	6.2%
Boeing 737-800	6.3%	Embraer EMB-145XR	2.0%
Boeing 737-900	1.0%	McDonnell Douglas MD-11	<1.0%
Boeing 747-400	<1.0%	McDonnell Douglas MD-82	2.4%
Boeing 757-200	5.5%	McDonnell Douglas MD-83	2.4%
Boeing 757-300	<1.0%	McDonnell Douglas MD-87	<1.0%
Boeing 767-200	<1.0%	McDonnell Douglas MD-88	2.7%
Boeing 767-300	<1.0%	McDonnell Douglas MD-90	<1.0%

3.6.2 CLIMB & DESCENT CORRECTION

Climbs and descents within the cruise phase are accounted for in the fuel burn analysis using a force-balance model illustrate in Figure 21. A multiplier to the level-flight thrust requirement is calculated based on the flight path angle of the aircraft. This model assumes that an aircraft in a climb or descent maintains the same Mach number as in level flight. In a climb,

* Frequency share is calculated with the 19-day ETMS sample set used in this study. This sample set includes flights with identifiable cruise segments above FL280 and occurring entirely within the CONUS. The numerator is the number of high-altitude operations for each type. The denominator is the total number of qualifying flights.

The sum of all frequencies reported above is 90.1%. The remaining 9.9% of high-altitude operations not accounted for in the table consist of about 100 other aircraft types, mostly GA.

the aircraft engines must produce thrust sufficient to overcome aerodynamic drag at the given speed as well as the component of weight parallel to the flight path of the aircraft. In a descent, the component of weight parallel to the flight path is in the direction of aircraft movement – less engine thrust is necessary to maintain a given speed than in level flight. Flight path angle (θ) is calculated for each 60-second segment of the cruise phase using the initial altitude, final altitude, and air distance travelled. Fuel burn rate is assumed to be proportional to engine thrust level.

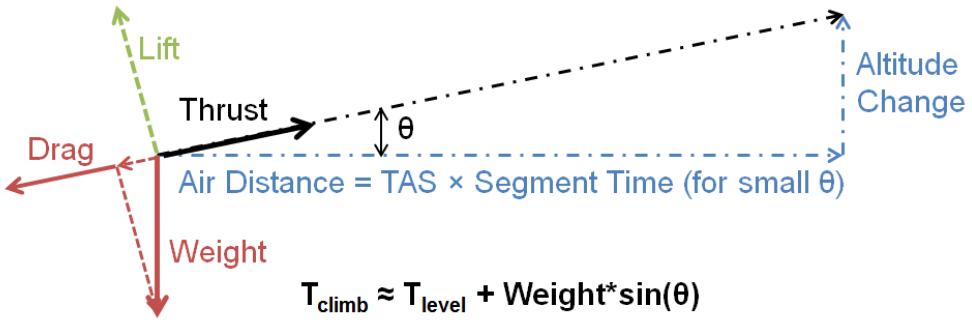

Figure 21. Force balance model used to account for fuel efficiency changes during climbs and descents

3.7 Trajectory Optimization: Altitude

For each flight in the sample set, trajectory data for the cruise phase is passed to the altitude trajectory optimizer. For altitude-only analysis assuming as-flown Mach, the procedure generates four alternative altitude optimal profiles including; (1) cruise climb; (2) 1000 ft increment step climb; (3) 2000 ft increment step climb; and (4) flexible VNAV altitude profile allowing climbs or descents with levels segments at 1000 ft increments. The method used for generating each profile is described below.

The altitude optimization algorithms all require that the baseline trajectory analysis has been run prior to implementation. During the baseline as-flown analysis, the instantaneous altitude efficiency profile is calculated at each one-minute interval along the cruise trajectory. Assuming constrained Mach, the expected SGR is calculated for each accessible altitude from 28,000 ft to the service ceiling of the aircraft. This calculation provides the expected fuel efficiency at every altitude under the hypothetical assumption that the aircraft could be positioned in level flight at any desired flight level at the current weight. Figure 22 illustrates the calculation of the altitude efficiency curve for a flight at a specific point in the cruise trajectory. This calculation accounts for wind and aircraft weight.

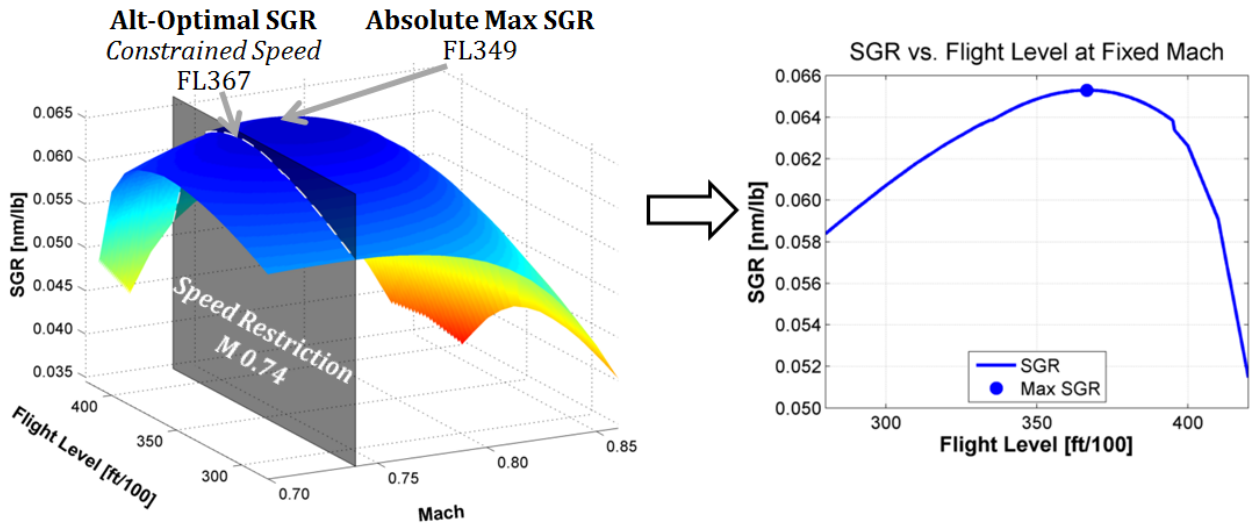

Figure 22. Illustration of instantaneous efficiency range for an aircraft with constrained speed and flexible altitude

The calculation of an instantaneous altitude efficiency function is repeated for every 60-second interval along the flight, accounting for changing wind speeds and aircraft weight. Improved altitude trajectories can be designed by analyzing this sequence of altitude efficiency curves over the full cruise phase of flight. Figure 23 shows a heat map visualization of this altitude efficiency sequence for a single example flight.

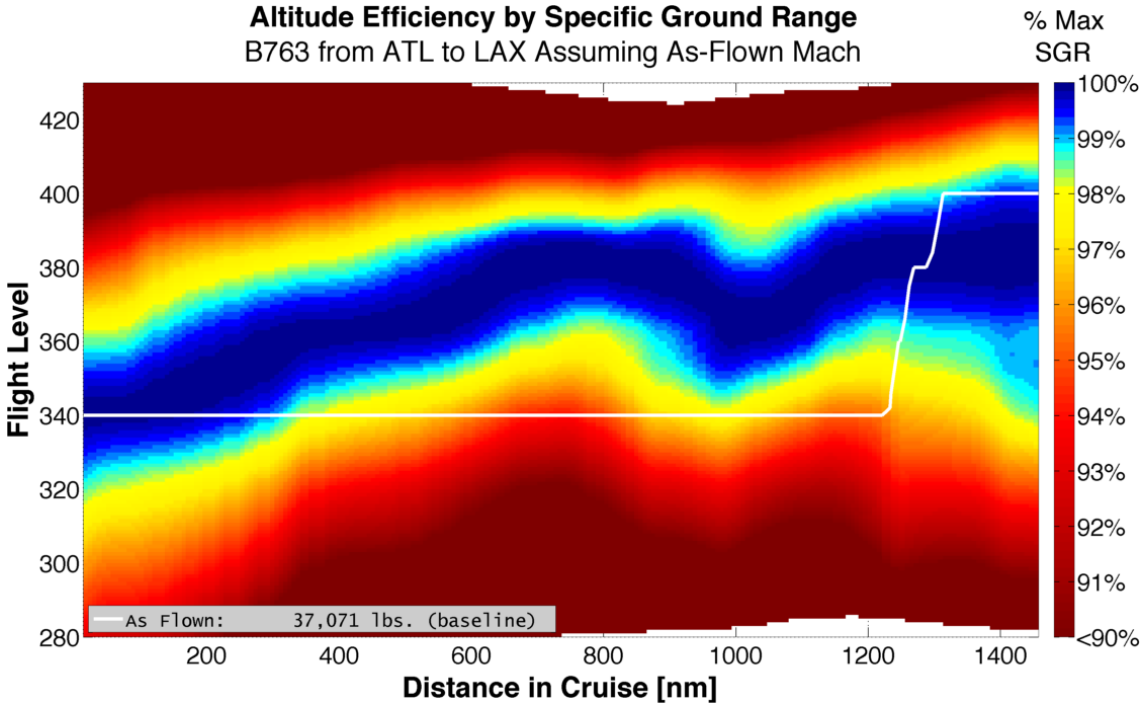

Figure 23. Altitude efficiency heat map showing SGR variation through the cruise phase with the baseline as-flown altitude profile shown in white

The heat map shows altitude efficiency as a percentage of the maximum-achievable value at every point in the cruise trajectory. This visualization illustrates some of the key considerations in planning optimal altitude profiles:

1) The optimal altitude fluctuates due to wind and temperature changes along the route of flight. This is interesting because in a no-wind environment with constant temperature, the optimal altitude profile is a constant-rate climb (optimal altitude increases with decreasing aircraft weight). Thus, while a constant cruise climb is widely assumed to be an optimal altitude profile in all conditions, the actual best profile is strongly dependent on weather.
2) The range of altitudes where efficiency is greater than 99% forms an optimal "tunnel", appearing in the heat map as the dark blue region. The width of this tunnel depends on aircraft type as well as atmospheric conditions.
3) Fuel efficiency falls off significantly as altitudes become farther from optimal. In this example, an altitude deviation 2000 ft below optimal causes a 3% efficiency loss. A larger deviation of 6000 ft causes an efficiency loss of more than 10%. Such deviations are commonly encountered in actual operations on account of ride quality or congestion.

Based on the data underlying the altitude efficiency heat map, it is possible to design a variety of improved altitude profiles to reduce cruise phase fuel consumption.

3.7.1 CRUISE CLIMB

The cruise climb optimizer is based on the locus of absolute optimal-efficiency altitudes for the full cruise phase of flight. This corresponds to the 100% efficiency band in Figure 23. Due to fine-scale variation in winds and temperatures combined with the shallow efficiency function near optimal altitudes, this set of absolute-optimal altitudes can be quite noisy and is generally not flyable. The cruise climb optimizer approximates the absolute optimal altitude using a least-squares linear regression, shown in Figure 24 for the same flight illustrated in Figure 23. The resulting trajectory has a constant rate of climb or descent.

All alternate altitude trajectories, including cruise climb, have a climb or descent enforced at the end of the segment to ensure potential energy parity between the baseline and optimized tracks. This is evident as a final climb at the end of the cruise-climb profile in Figure 24. Without this adjustment, fuel burn benefits or drawbacks could be attributed to altitude optimization when in fact the optimized profile had more (or less) total potential energy change than the baseline trajectory. The final altitude adjustment ensures that an equal portion of the fuel burn estimate for every optimized trajectory can be attributed to potential energy change.

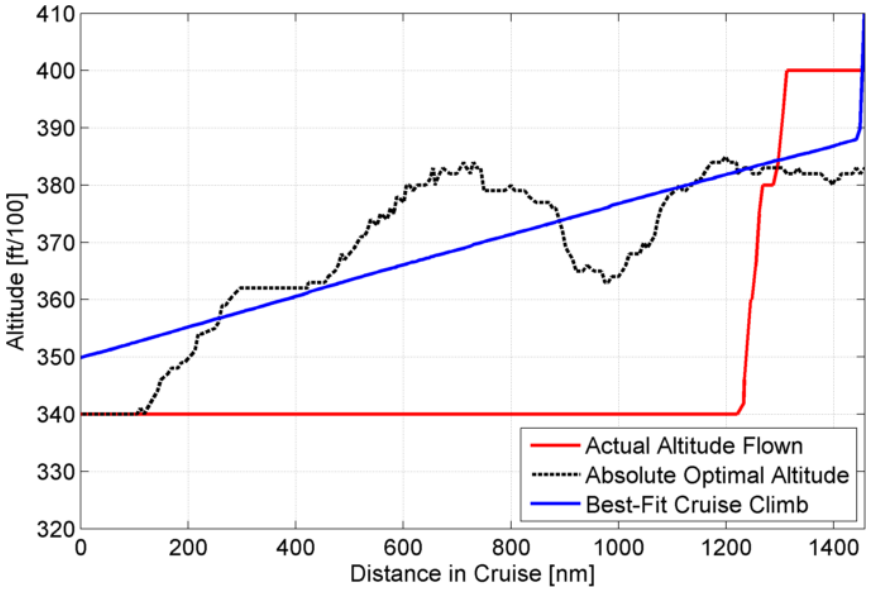

Figure 24. Illustration of cruise climb altitude optimization using least-squares linear regression

3.7.2 STEP CLIMB

Step climb profiles are based on the output of the cruise climb optimizer. The cruise climb altitude profile is simply rounded to the nearest 1000 ft or eligible 2000 ft level, as shown in Figure 25. For 2000 ft altitude optimization, standard RVSM equipage is assumed. Eastbound flights are constrained to odd-thousand altitudes (i.e. FL330, FL350, and FL370) while westbound flights are constrained to even-thousand altitudes (i.e. FL340, FL360, FL380).

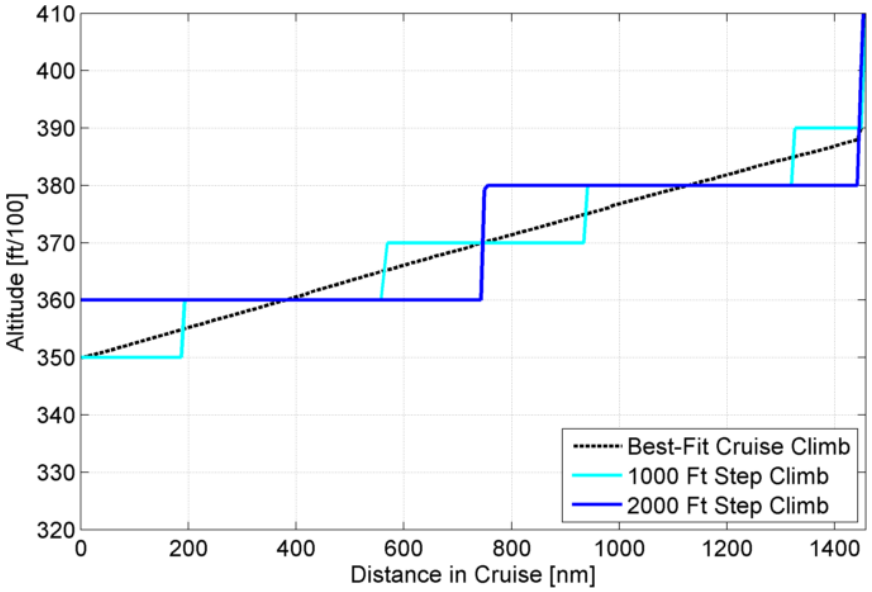

Figure 25. Illustration of step climb altitude optimization

3.7.3 FLEXIBLE VNAV

The Flexible VNAV altitude optimizer generates trajectories that require level cruise segments at 1000-ft increments but otherwise provides significant flexibility for tracking fuel-optimal altitudes throughout the cruise phase. This trajectory uses the Dijkstra graph search algorithm to find the lowest-cost route through a two-dimensional graph weighted by fuel efficiency at each altitude. The graph of potential altitude profiles is constructed such that each point is connected to at most five other points: the next waypoint at the same altitude, or a waypoint a specified number of minutes later at an altitude 1000 ft or 2000 ft above or below the current altitude. This constrains the problem so the trajectory may include a climb or descent from any point, but a climb or descent is always followed by a period of level flight. In this study, the minimum level flight threshold is set at 10 minutes. The starting point for the flexible VNAV trajectory is the most-efficient 1000-ft altitude level at the beginning of the cruise phase. This graph structure is illustrated in Figure 26. The initial waypoint is connected to five possible paths, shown with solid black lines. The endpoints of the first step, shown as solid black dots, can then be connected to up to five more points. Two of the five such branch points are shown in the figure as dashed black lines.

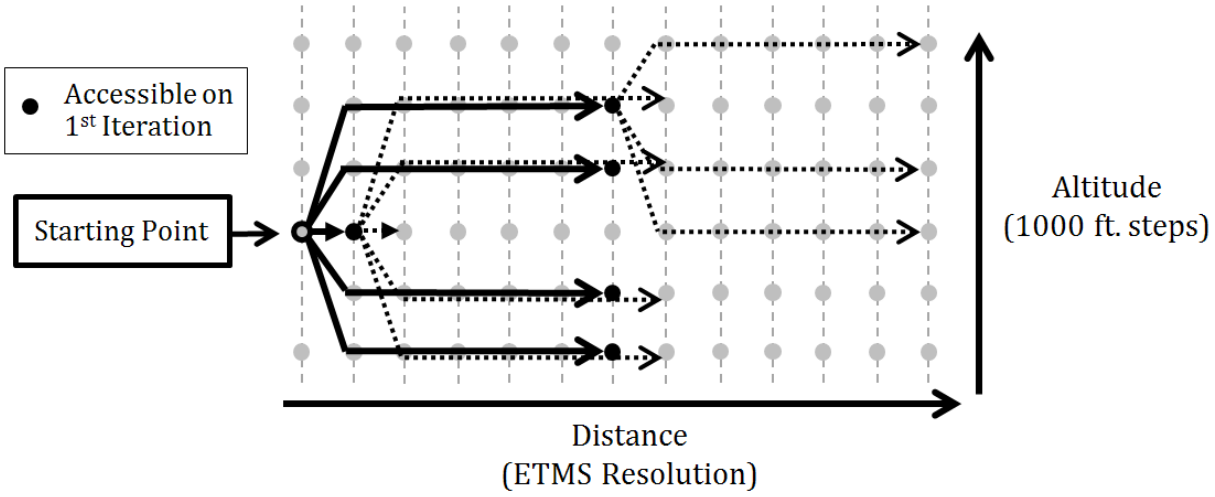

Figure 26. Flexible VNAV graph structure (first two steps) for use with the Dijkstra minimum-cost path algorithm

Weighting is applied to each potential connection in the graph structure based on the altitude efficiency values. By minimizing the total cost of traversing the graph from the start to the end of cruise, an optimal VNAV profile is defined. Figure 27 shows the flexible VNAV altitude optimizer output overlaid on the absolute optimal altitude track. This method is more intricate than the regressions and closest-fit heuristics used for cruise climb and step climb analysis because it takes into account the efficiency levels away from the optimal altitude. Any flyable trajectory requires some periods of off-optimal cruise altitude. This method accounts for and minimizes these periods. Therefore, the output shown in Figure 27 considers the efficiency both on and around the absolute optimal altitude.

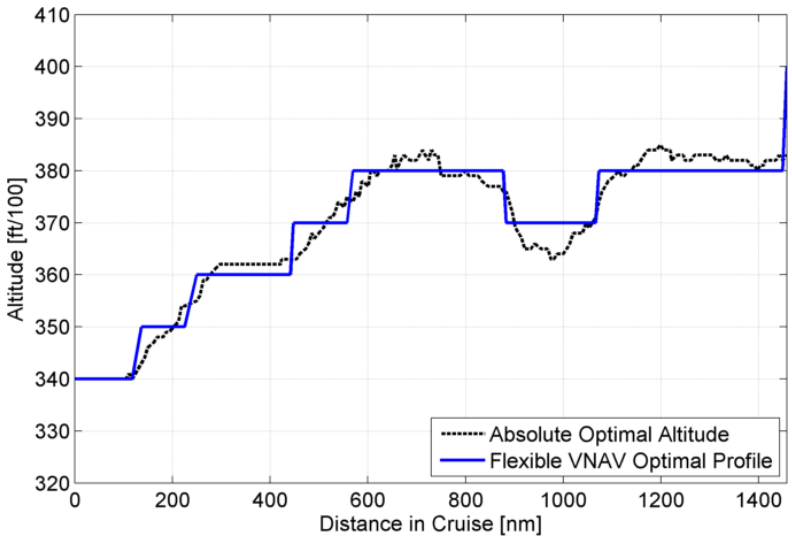

Figure 27. Illustration of flexible VNAV altitude optimization output

3.8 Trajectory Optimization: Speed

Each cruise trajectory is processed by the speed optimizer independently from the altitude optimizer. For speed-only analysis assuming as-flown altitude, the procedure generates three alternative altitude optimal profiles including; (1) MRC; (2) LRC; and (3) LRC or actual. The method used for generating each profile is described below.

Unlike the altitude optimizers, which require altitude efficiency fields as initial inputs, the speed optimization algorithms do not require that baseline trajectory analysis has been completed prior to implementation. For each one-minute interval along the cruise segment, the efficiency at every speed between Mach 0.70 and the maximum speed of the aircraft is calculated assuming as-flown altitude. This speed efficiency curve is then used to determine the absolute optimal speed (MRC) and the faster speed where efficiency is 99% of optimal (LRC) as shown in Figure 28. The procedure accounts for the aircraft weight and actual winds at each point along the trajectory.

Changes in speed impact the flight time for a cruise segment. Therefore, in addition to outputting expected fuel burn for each interval in the original ETMS record, the speed optimizer also updates the elapsed time for each interval in sequence. This shifts the calculation time at the next interval, potentially changing the wind experienced at that location. The time adjustments compound through all the intervals in the cruise phase, ultimately outputting an expected flight time change as a result of speed optimization.

The "LRC or actual" optimization profile recognizes that many flights operate more efficiently than LRC in the baseline case. Therefore, this optimization applies an LRC optimization only when it improves upon baseline fuel efficiency. Otherwise, the as-flown speed profile is maintained.

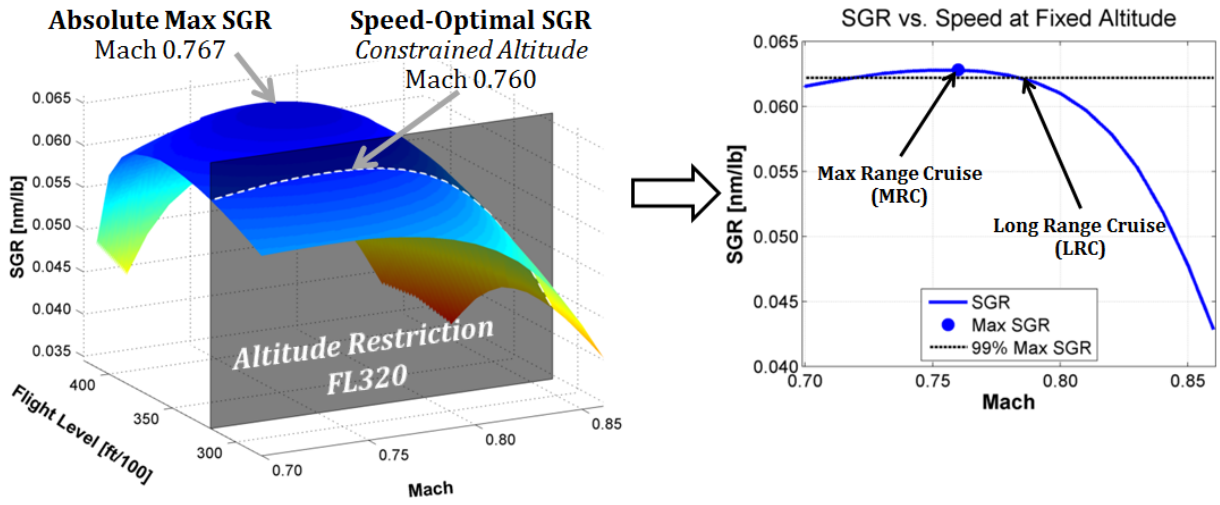

Figure 28. Illustration of instantaneous efficiency range for an aircraft with constrained altitude and flexible speed

3.9 Trajectory Optimization: Joint Altitude & Speed

The joint optimizer finds optimal trajectories given flexibility in both speed and altitude. A single joint-optimal trajectory is generated for each flight in the sample set. This is a two-step method, first generating optimal tracks with no constraints and then enforcing flyability on those tracks using a shortest-path graph search implementation. First, the absolute optimal speed and altitude are calculated for each interval in the cruise segment in much the same manner as for the previous optimizers but without constraints. This optimal point corresponds to the global maximum on the efficiency surface shown in Figure 22 and Figure 28. The speed in each interval is used to calculate flight time impacts similar to the case for speed optimization. In addition to calculating the optimal speed and altitude for each interval in cruise, the fuel efficiency is also recorded at each combination of speed (0.01 Mach resolution) and altitude (1000 ft resolution).

These absolute optimal trajectories tend to be noisy in both speed and altitude. In order to ensure flyability, frequent altitude and speed changes are not permissible. Therefore, each track is processed a second time with the absolute optimal results as an input. A graph search methodology similar to that for the Flexible VNAV altitude optimizer is used to find the optimal flyable path. The graph is constructed such that altitude changes are allowed only after 10 minutes or more of level flight and speed changes are limited to 0.01 Mach per cruise interval. A simplified representation of the graph is shown in Figure 29.

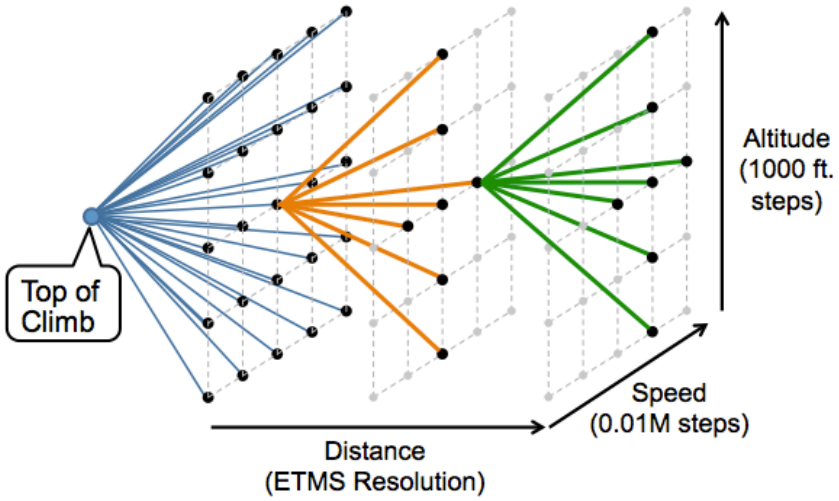

Figure 29. Simplified representation of joint altitude and speed optimization graph structure for application of Dijkstra's Algorithm

The graph is weighted based on the fuel efficiencies at each combination of speed and altitude. Using these efficiency weightings and a graph structure reflecting flyability constraints, the Dijkstra shortest-path algorithm is applied to find the minimum cost solution to traverse the full cruise phase.

Page Intentionally Left Blank

Chapter 4 RESULTS

4.1 Altitude Optimization Results

The full set of sample flights was analyzed using the procedure outlined in Section 3.7. Outputs were generated for four optimal profiles on each flight: cruise climb, 1000 ft step climb, 2000 ft step climb, and flexible VNAV. For each of these profiles, the following results were stored:

- Optimal altitude at every interval along the ETMS cruise track
- Estimated fuel burn reduction relative to the baseline trajectory (lbs and percent)
- Instantaneous fuel efficiency at every interval along the ETMS cruise track (SAR and SGR)
- Estimated flight time impact of modified altitudes relative to the baseline trajectory (minutes and percent)
- Altitude efficiency heat map showing the relative efficiency of all possible altitudes along the cruise track

Results from a selection of five individual flights are presented here to illustrate some of the important factors involved with altitude optimization. These examples - drawn from a variety of days, airlines, and aircraft types - show the significant variation in optimal altitude profile between flights.

4.1.1 INDIVIDUAL FLIGHT ALTITUDE RESULTS

Figure 30 shows results for a representative medium-range flight in the NAS operated by a Boeing 757-200. The baseline altitude trajectory flown by the aircraft, shown in white, began at FL360. Midway through the flight, the aircraft descended to FL340, before stepping down to FL320 for the final 200nm of the cruise phase. The optimal altitude tunnel, shown as dark blue in the background heat map, indicates that this step-down reduced the fuel efficiency of the flight. Had the aircraft flown optimal 1000-ft cruise levels throughout the flight (flexible VNAV optimization, shown as dashed blue in the figure), the cruise fuel savings would have been 1.70%. The 2000-ft step climb optimal (shown as solid red in the figure) would have provided a 1.53% fuel burn savings while complying with directional RVSM altitude constraints.

The optimal altitude tunnel for this aircraft gets significantly narrower near the end of the flight. Thus, as the aircraft flew farther from optimal altitudes, the altitude sensitivity was actually increasing. From an efficiency standpoint, it was more important for this flight to be near optimal at the end of the flight than at the beginning. In actuality, the SGR was 6% below optimal by the end of the cruise phase.

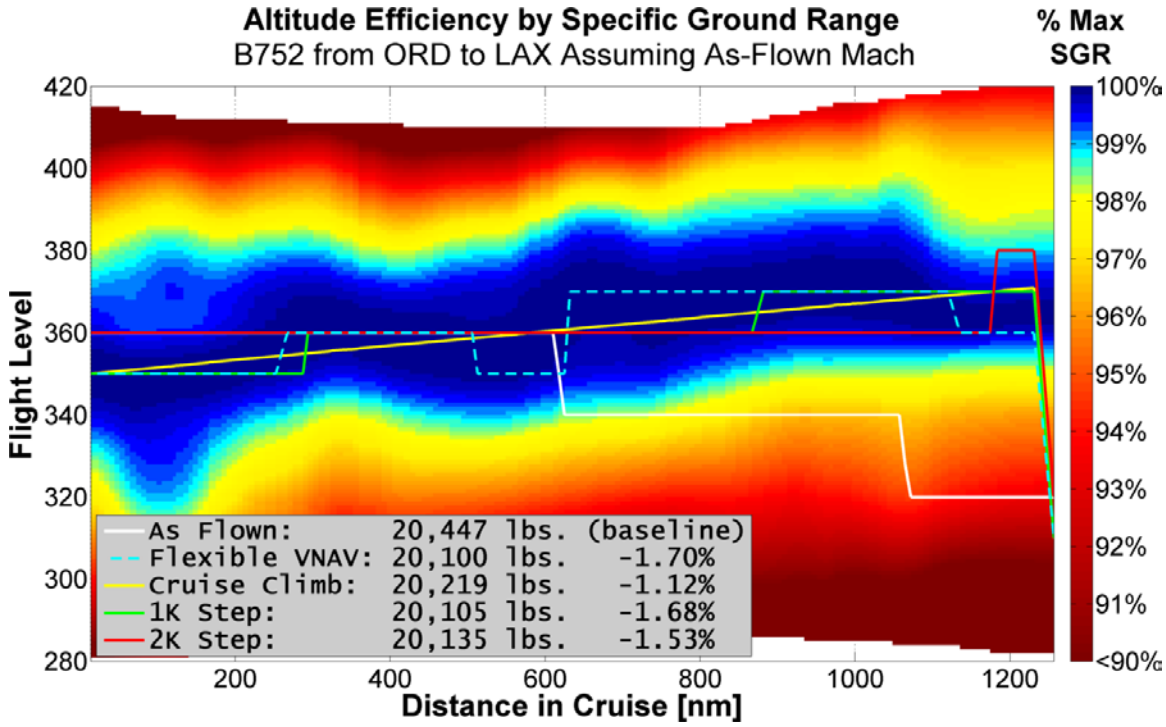

Figure 30. Sample altitude output: B757-200 from Chicago to Los Angeles

Figure 31 shows results for another medium-range flight operated by a Boeing 737-900. The optimal altitude tunnel shows a pronounced increase in width midway through the flight. The as-flown trajectory includes a descent to FL280 between 400nm and 750nm into the cruise. 750nm into its cruise phase, the flight climbed briefly to FL360 before returning to FL340 for the remainder of its cruise. Despite the aggressive altitude change executed by the flight between 400nm and 750nm, the total fuel saving potential from flexible VNAV altitude optimization is only 1.37%. At no point in the trajectory was the aircraft operated at an efficiency more than 5% below its optimal SGR.

Figure 32 shows results for a short-range flight operated by the Bombardier CRJ-200. The optimal altitude tunnel shown by the altitude efficiency heatmap suggests a large window of optimal altitudes on this flight. However, the as-flown trajectory is below the optimal level throughout the cruise phase. The flight initially cruised at FL310 before climbing to FL330, despite optimal altitudes some 6,000-8,000 ft higher. On this flight, the potential fuel savings from flexible VNAV optimization was 3.91%. The cruise climb benefit was slightly higher at 3.94%. All of the optimal profiles are significantly different than the as-flown baseline.

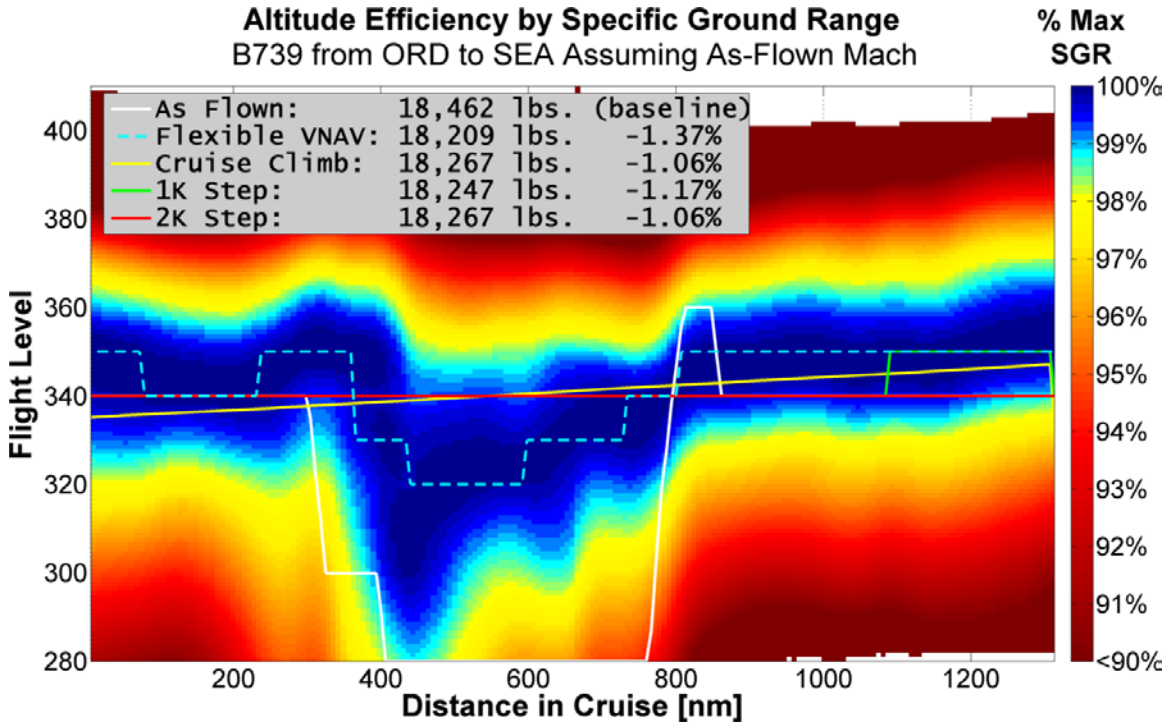

Figure 31. Sample altitude output: B737-900 from Chicago to Seattle

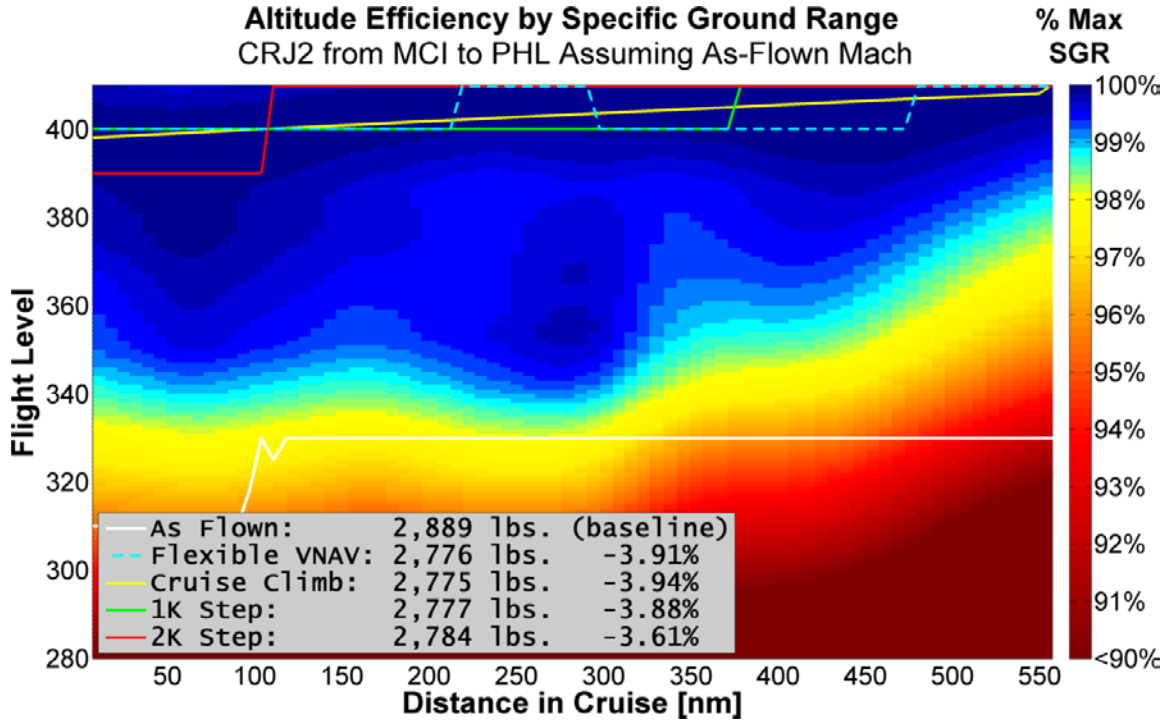

Figure 32. Sample altitude output: CRJ-200 from Kansas City to Philadelphia

Both Figure 33 and Figure 34 show flights with profiles that are approximated closely by traditional constant-rate cruise climbs. One is a short-range flight operated by a CRJ-700 and the other is a medium-range flight operated by an Airbus A321. The two figures clearly show the differences in optimal altitude ranges between aircraft types. In both cases, the as-flown profile was a single altitude throughout the cruise phase. In the case of the CRJ-700 flight shown in Figure 33, the initial altitude was higher than optimal but became close to optimal as the flight progressed. For the A320 flight shown in Figure 34, the initial altitude was initially efficient but became less so as the flight progressed and the aircraft became lighter. In both cases, fuel burn reduction of more than 1% would have been possible with optimal altitude trajectory design.

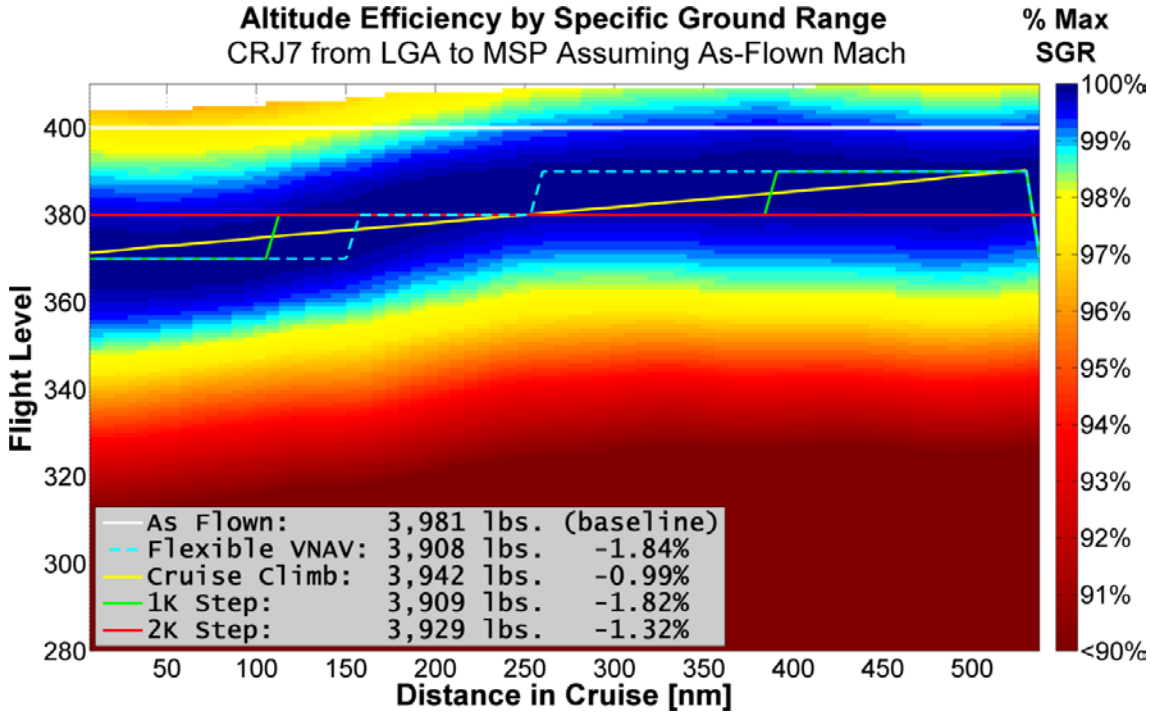

Figure 33. Sample altitude output: CRJ-700 from New York (La Guardia) to Minneapolis

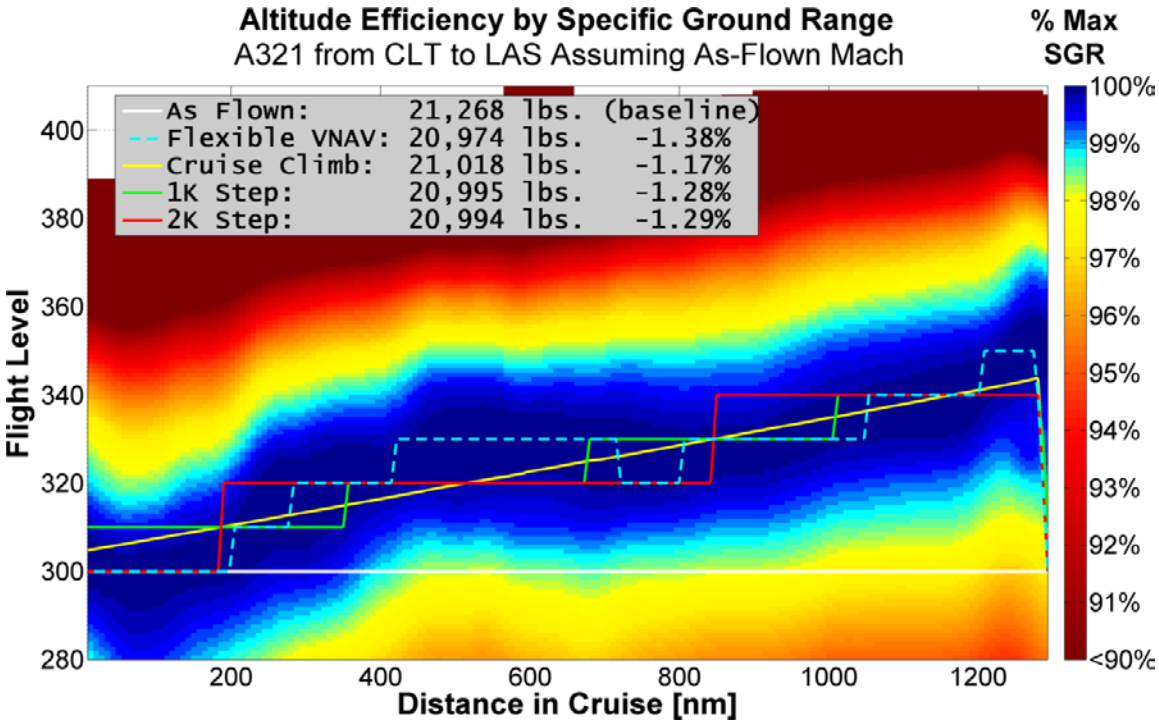

Figure 34. Sample altitude output: A321 from Charlotte to Las Vegas

4.1.2 AGGREGATE ALTITUDE RESULTS

The individual flight analysis presented in section 4.1.1 was repeated for the full sample set of 217,000 flights in 2012. The distribution of results for the 2000 ft step climb optimizer are shown in Figure 35. This profile constrains flights to the directional RVSM flight levels shown in Figure 3. This constraint reflects current operating practices in the NAS, reducing barriers to implementation relative to the other optimization profiles.

It is immediately apparent from the distribution of altitude results that most flights already operate relatively near the optimal altitude point. 33% of flights had potential optimization benefits between 0% and 0.5% of optimal. Thus, one out of three flights already operated very close to the optimal profile. Many of those flights are those that operated the optimal altitude profile in the baseline case, thus making the optimized trajectory identical to the baseline. This is particularly common on shorter flight legs, where the 2000 ft step climb profile is frequently a single altitude level throughout the cruise phase – a condition that is quite simple to match in actual operating conditions.

Conversely, the result distribution also shows the significant portion of the output set that operates very far from optimal altitudes. The top quartile (25%) of flights with the greatest optimization potential from 2000 ft step climbs all have greater than 4.61% expected fuel burn reduction. By targeting those flights with especially large fuel burn reduction potential, the impact of CASO can be much larger than by attempting to optimize those flights already operating near optimal.

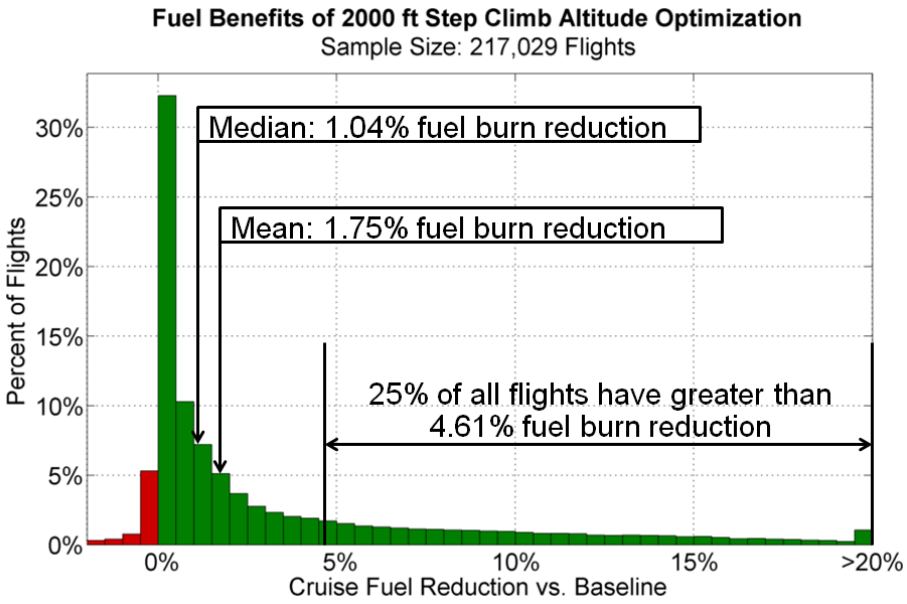

Figure 35. Aggregate fuel burn reduction from 2000 ft step climb altitude optimization

The distribution shows a mean fuel burn reduction from 2000 ft step climb implementation across all flights of 1.75% with a median at 1.05% fuel burn reduction. While the 2000 ft step climb profile is the most representative of what can be implemented quickly, it also has the lowest potential benefits of all the optimization techniques. The distribution of results for Flexible VNAV altitude optimization is shown in Figure 36.

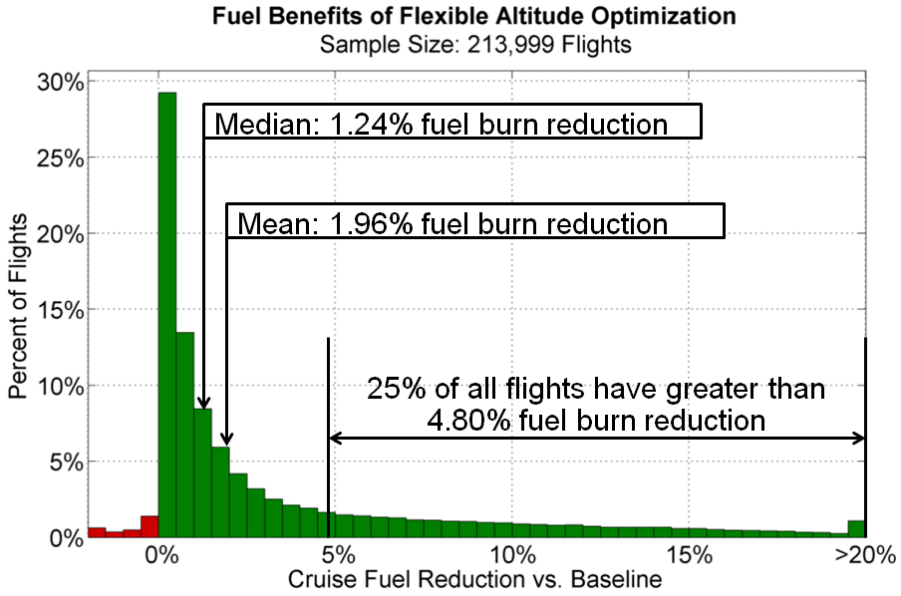

Figure 36. Aggregate fuel burn reduction from flexible VNAV altitude optimization

The average fuel burn reduction with Flexible VNAV altitude potential is 1.96% with a median of 1.24%. The top 25% of flights with the highest benefit potential all saw a fuel burn reduction of 4.80% or greater. While these results improve upon the 2000 ft step climb results by an average of 0.19% per flight, the difference in complexity between the two profile definitions is significant. In order to fly a flexible VNAV altitude profile, 1000 ft altitude increments must be available and pilots need access to high-fidelity wind models. The 2000 ft step climb is a simpler solution offering comparable results to the flexible VNAV optimizer.

Figure 37 and Figure 38 show the fuel burn reduction distributions for the cruise climb and 1000 ft step climb altitude profiles, respectively. Both profiles have similar characteristics, including strong clustering of results near low-benefits conditions with a significant distribution tail containing high-benefit operations.

Comparing cruise climb and 1000 ft step climb results distributions, there is no incremental benefit of cruise climbs compared to step climbs. The step climb average fuel burn reduction is 0.03% higher than the cruise climb value, while the high-benefits tail of the distribution is also shifted slightly further to the right in the figure. For practical purposes, the two distributions have nearly identical characteristics except for the relatively high number of negative results indicated by the cruise climb altitude optimizer. These are caused by the cruise climb altitude profile (constrained to be a constant-rate climb) passing through localized pockets of poor efficiency that were avoided in the baseline trajectory.

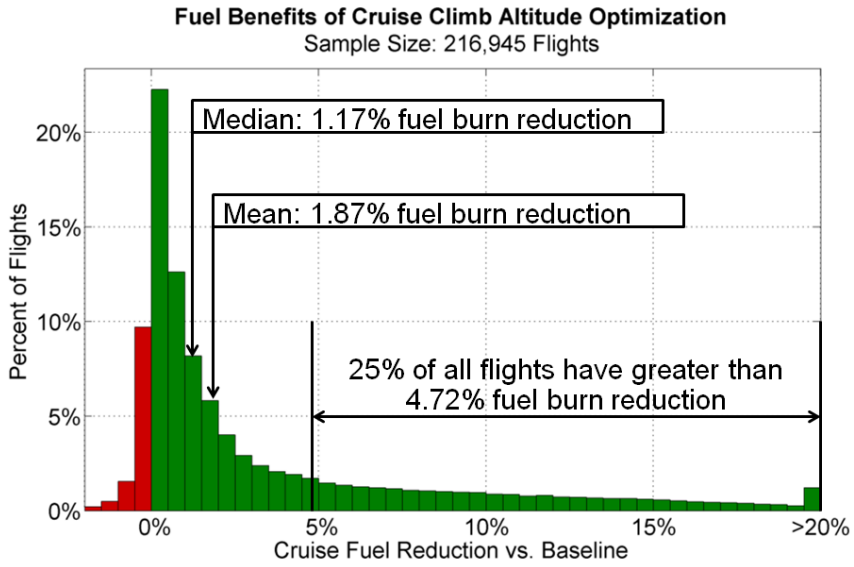

Figure 37. Aggregate fuel burn reduction from cruise climb altitude optimization

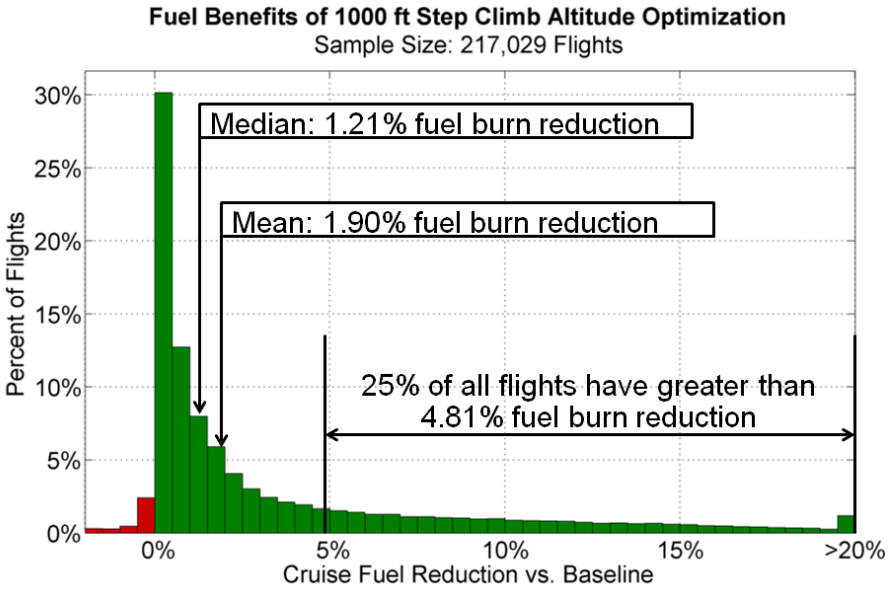

Figure 38. Aggregate fuel burn reduction from 1000 ft step climb altitude optimization

Results for fuel burn reduction across all flights for each type of altitude optimization are given in Table 4, further broken down by stage length. The absolute fuel saving results (reported in pounds) represent the mean fuel burn reduction relative to the as-flown trajectory. The percentage results are calculated as the ratio of mean fuel burn reduction potential to mean total cruise fuel burn in the baseline trajectory for the same set of flights.

Table 4 shows that the Flexible VNAV altitude optimizer resulted in the largest fuel burn reduction of all optimization methods for each stage length. This was expected because the trajectories generated by this optimizer follow the optimal altitude tunnel discussed in Section 4.1.1 more closely than the other optimized profiles.

All of the altitude optimization methods resulted in average fuel burn reduction potentials between 1.75% and 1.96%. This represents a difference of 11 lbs of incremental fuel savings per flight by moving from 2000 ft. step climbs (the worst performing optimization) to flexible VNAV profiles (the best performing optimization). The absolute value of fuel reduction potential ranges from 96 lbs per flight (for the 2000 ft step climb optimizer) to 107 lbs per flight (for the flexible VNAV optimizer).

Table 4. Aggregate Altitude Optimization Results

Stage Length[†]	Mean Cruise Fuel Burn Reduction			
	Cruise Climb	**1000 ft Step Climb**	**2000 ft Step Climb**	**Flexible VNAV**
0-500 nm *n=67,486*	86 lbs 5.74%	87 lbs 5.80%	84 lbs 5.63%	87 lbs 5.80%
500-1000 nm *n=109,971*	83 lbs 1.83%	87 lbs 1.90%	80 lbs 1.75%	88 lbs 1.93%
1000-1500 nm *n=24,757*	158 lbs 1.40%	161 lbs 1.42%	144 lbs 1.28%	171 lbs 1.51%
1500-2000 nm *n=9,837*	204 lbs 1.10%	205 lbs 1.11%	176 lbs 0.95%	228 lbs 1.23%
2000-2500 nm *n=4,491*	244 lbs 0.94%	242 lbs 0.93%	201 lbs 0.77%	278 lbs 1.07%
Total	**102 lbs** **1.87%**	**104 lbs** **1.91%**	**96 lbs** **1.75%**	**107 lbs** **1.96%**

On average, shorter stage lengths had significantly larger percentage fuel burn benefits from altitude optimization than longer stage lengths. The absolute fuel burn on these segments was relatively small because of the short length of the cruise phase. For Flexible VNAV optimization, the mean potential fuel burn reduction for flights less than 500nm in length was 5.80%. This compares to mean values ranging from 1.07% to 1.93% for longer stage lengths. Because a full 32% of the analysis set falls within this short range grouping, there appears to be a strong trend of inefficient operations in short-haul operations with a large number of flights contributing to that trend. Absolute fuel burn savings in pounds grow in proportion with the average stage length.

4.1.3 DIFFERENCES BETWEEN AIRLINES AND AIRCRAFT TYPES

The output set was broken down further by airline and by aircraft type to better classify systemwide altitude efficiency characteristics. Figure 39 shows the efficiency performance for the ten airlines with the highest flight count in the output set.

The airlines are classified as mainline or regional based on fleet mix and sales/distribution channels used for tickets. The airlines marked as mainline carriers all market and sell tickets under their own brand names and fly aircraft with more than 100 seats. The airlines marked as regional carriers do not market and sell tickets under their own brand names and do not operate aircraft types carrying more than 100 passengers.

[†] Stage length refers to the great circle distance from the origin airport to the destination airport

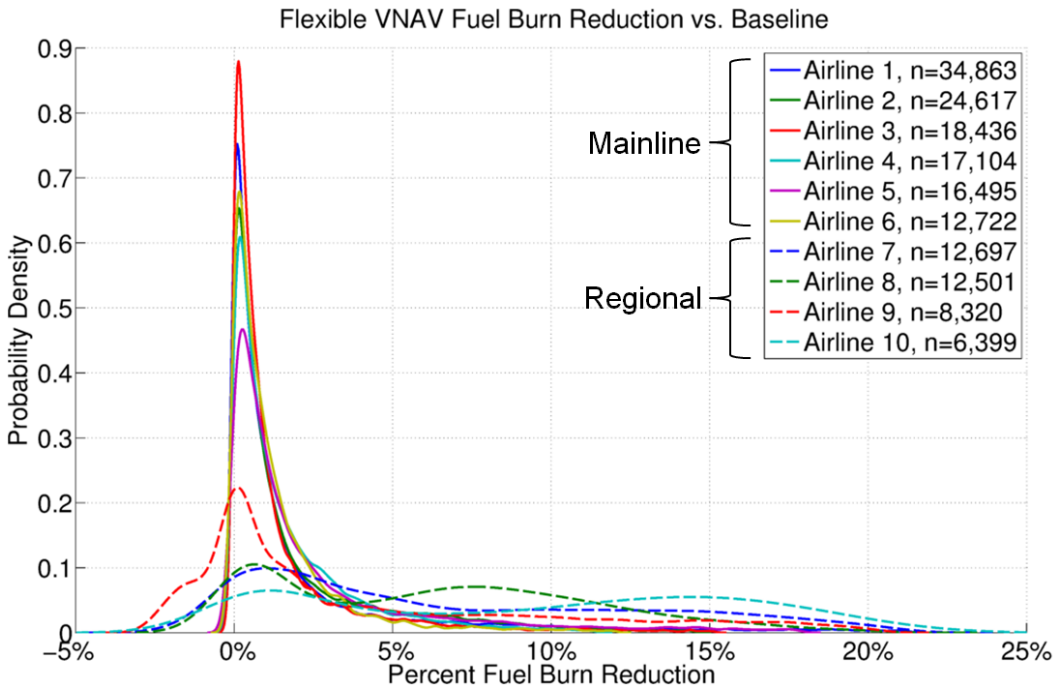

Figure 39. Distribution of benefits from flexible VNAV altitude optimization for the 10 most common airlines in the output set

The altitude efficiency performance for each airline is presented as a probability density function (PDF). Efficient operations are characterized by sharp peaks near 0%, indicating that the majority of flights for the given airline already operate near fuel-optimal altitudes. Airline 3 is an example of such an efficient distribution. Distributions showing greater probability density at higher percentage benefits and with lower peaks near the 0% point correspond to airlines that currently operate far from optimal altitude trajectories. The distribution for airline 10 is an example of a highly inefficient operation, with a significant number of flights operating with 15% or greater fuel reduction potential from altitude optimization.

From the figure, it is clear that regional airlines perform less optimally than mainline carriers in terms of altitude efficiency. This pattern holds for all regional and mainline carriers. The lowest-performing mainline carrier (Airline 5) still has a significantly more efficient distribution than the best-performing regional carrier (Airline 9). In order to better understand the reason for the differences between airlines, it is important to examine differences between aircraft types.

Figure 40 shows the efficiency performance for the ten aircraft types with the highest flight count in the output set. These results are also divided into regional and mainline fleet types based on aircraft seating capacity. Types with more than 100 seats were classified as mainline, while those with fewer than 100 seats were classified as regional. As was the case for airline

analysis, altitude efficiency of the regional aircraft is much worse than the mainline aircraft on most services. The CRJ-200 appears to have particularly poor altitude efficiency on average, with very few flights operating near the optimal altitude for that aircraft. Of the mainline aircraft types included in the output set, the B737-800 has the most efficient distribution while the B737-300 operated farthest from optimal of the types included in the figure.

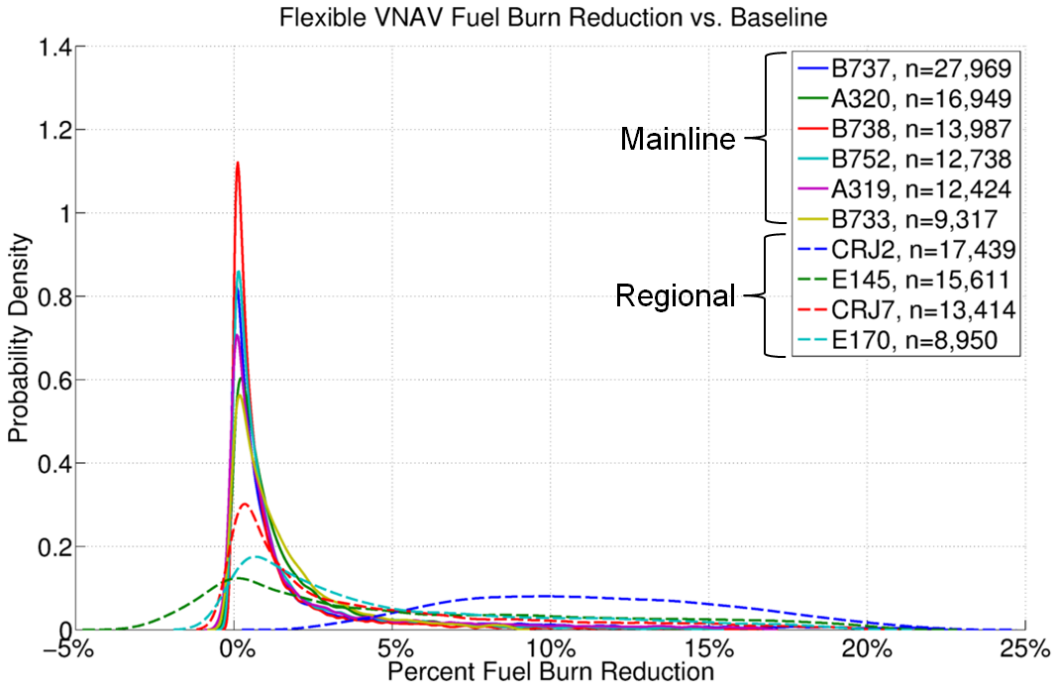

Figure 40. Distribution of benefits from flexible VNAV altitude optimization for the 10 most common aircraft types in the output set

4.2 Speed Optimization Results

In parallel with altitude analysis, the full set of sample flights was analyzed using the procedure for speed optimization outlined in Section 3.8. Outputs were generated for two alternative profiles on each flight and one hybrid profile: MRC, LRC, and "LRC or better". The structure and content of the output set is the same as for the altitude cases.

Results from a selection of four individual flights are presented here to demonstrate some common characteristics and variations in cruise speed optimization profiles. The examples are taken from a variety of days, airlines, aircraft types, and stage lengths. In each case, the baseline profile is plotted along with LRC and MRC optimized speeds.

4.2.1 Individual Flight Speed Results

Figure 41 shows speed optimization profiles for a flight from Dallas to Miami operated by a B737-800. The baseline speed ranged from Mach 0.78 to Mach 0.81. The maximum cruise speed

for the B737-800 is Mach 0.82. The MRC optimal cruise speed ranged from Mach 0.755 at the beginning of the cruise phase to Mach 0.745 at the end. The LRC speed trajectory followed a similar trend to the MRC trajectory offset by Mach 0.02. The fuel reduction potential was 4.58% for MRC is and 3.59% for LRC, a difference of almost exactly 1% as implied by the definition of LRC. Compared to the baseline flight, the LRC optimized version would have required an extra 2.2 minutes in cruise compared to an extra 5.0 minutes for the MRC optimal trajectory.

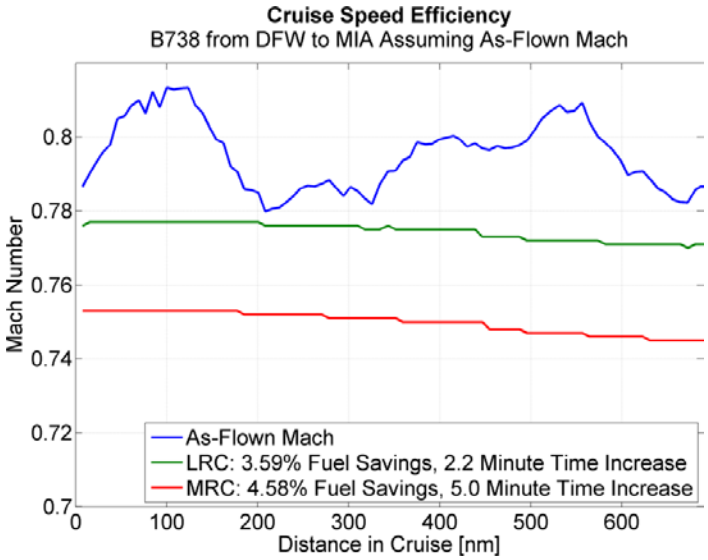

Figure 41. Sample speed output: B737-800 from Dallas to Miami

Figure 42 shows results for a flight from Houston to Seattle operated by a B757-200. This example differs from the first in that the baseline flight did not fly faster than the LRC speed throughout the entire cruise phase. About half way through the flight, the speed dropped below the LRC speed, at times dropping nearly to MRC speed. Despite these reductions in speed to near-optimal levels for parts for of the cruise phase, there was still a net potential fuel savings for both LRC (0.29% fuel reduction) and MRC (1.29% fuel reduction) optimization. The LRC profile has nearly the same duration as the baseline, while the MRC profile would require an additional 5.7 minutes due to reduced speed.

Figure 43 and Figure 44 provide two more sample trajectories illustrating different possible behaviors for baseline and optimized speed profiles. In Figure 43, a B737-300 flight appears to have slowed gradually throughout the cruise, ranging from about Mach 0.76 at the beginning of cruise to Mach 0.72 at the end of cruise. It is interesting to note that the optimal speed increased throughout the cruise phase on this flight, opposite from the normal behavior of gradually reduced optimal cruise speed as the aircraft becomes lighter. Such behavior is driven by increasing headwind through the flight. Figure 44 shows a flight operated by an MD-88 where the baseline trajectory was faster than optimal throughout the cruise phase of the flight. The output from this flight is interesting because the MRC and LRC optimal profiles are not parallel through the full duration of cruise. MRC speed drops by 0.01 Mach over the course of cruise

while the LRC speed stay nearly constant. Despite these differences, the output fuel reduction potential from the two optimized profiles are roughly equivalent.

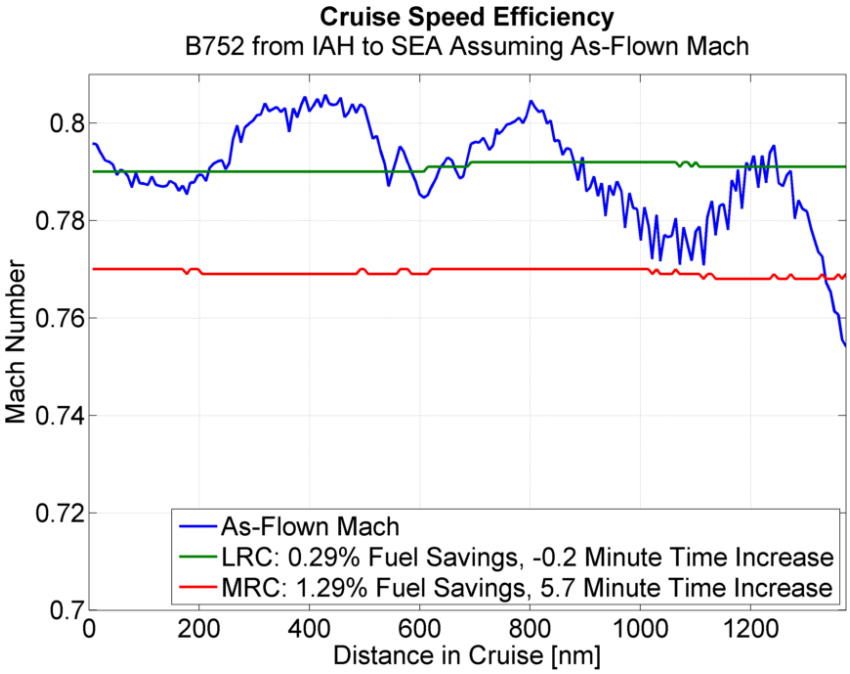

Figure 42. Sample speed output: B757-200 from Houston to Seattle

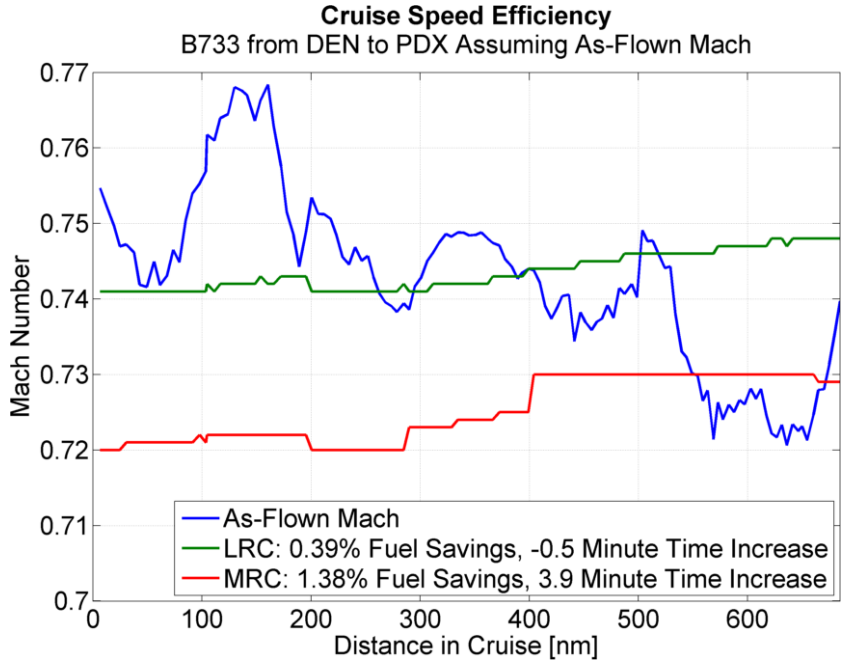

Figure 43. Sample speed output: B737-300 from Denver to Portland

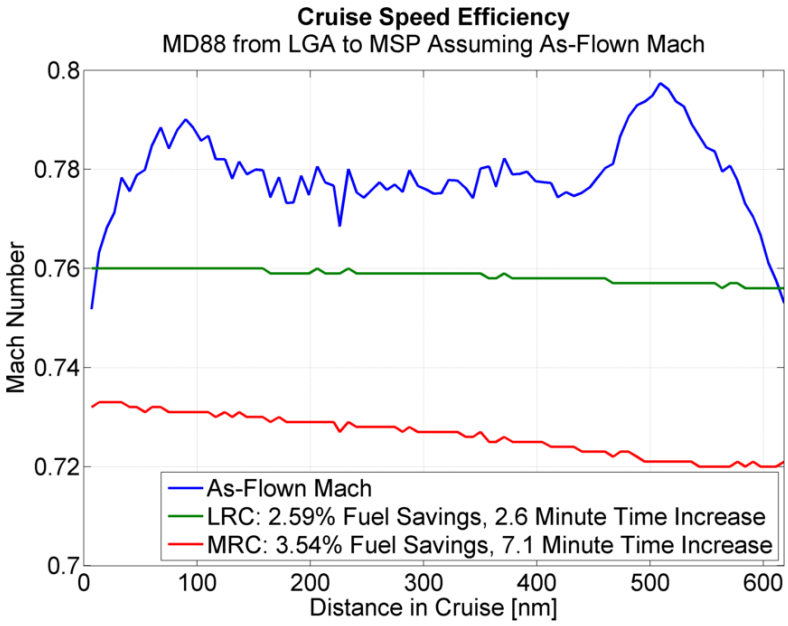

Figure 44. Sample speed output: MD-88 from New York (La Guardia) to Minneapolis

4.2.2 AGGREGATE SPEED RESULTS

The distribution of MRC speed optimization results across all flights is shown in Figure 45. The mean fuel burn reduction is 1.96% with a median benefit of 1.24%. As was evident in the altitude optimization results, many flights already operated close to optimal speeds. However, the highest-benefit 25% of flights all have greater than 2.83% fuel burn reduction potential. The distribution tail for speed optimization does not include as many flights with extremely large fuel burn benefits as in the altitude profiles. There are very few examples of flights with greater than 10% fuel burn reduction potential from MRC speed optimization.

The distribution of LRC fuel burn optimization benefits is shown in Figure 46. The mean fuel burn benefit for all flights of 0.93% with a median of 0.39%. The striking feature of the LRC benefits distribution is the large portion (nearly 40%) of flights with a fuel burn increase relative to the baseline trajectory. These flights represent those that were operated more efficiently than LRC speed, so LRC speed optimization entails increasing speed and decreasing fuel efficiency. The highest-benefit 15% of operations still have 1.82% or greater fuel burn optimization potential.

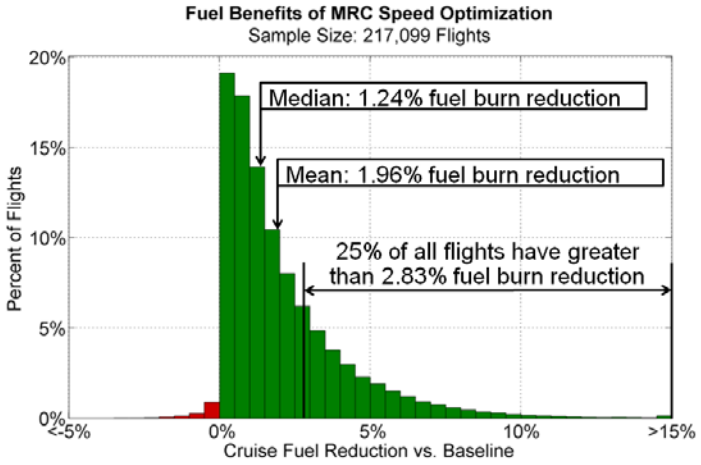

Figure 45. Aggregate fuel burn reduction from MRC speed optimization

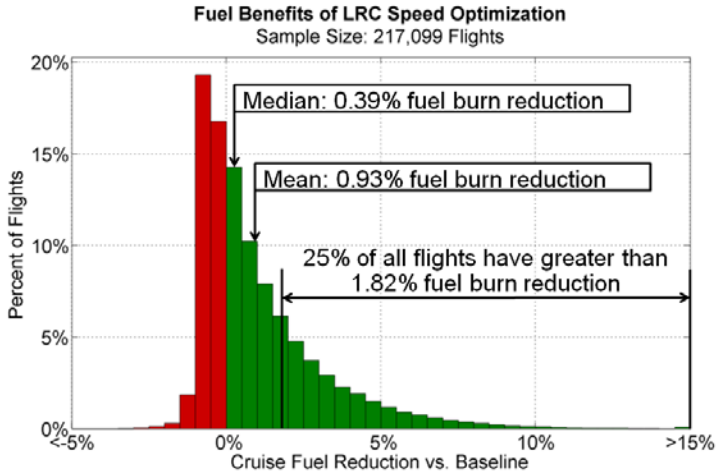

Figure 46. Aggregate fuel burn reduction from LRC speed optimization

It is counterproductive that flights at speeds more efficient than LRC are assumed to speed up in an LRC optimization program. Assuming that such flights maintained their baseline speed profile, but all flights that could benefit from the change switched to LRC speed, the average benefit for all flights increases from 0.93% to 1.13%. This "LRC or Actual" speed optimization is more implementable than either standalone MRC or LRC.

Another key aspect of speed optimization is that slowing down to conserve fuel causes flight time to increase. It is important to understand the magnitude of this time increase relative to expected fuel reduction. Figure 47 shows the distribution of flight time change relative to the baseline trajectory due to altitude optimization (in minutes) for both LRC and MRC optimization.

The results provide insight into the reason LRC may be preferable to MRC from an airline standpoint. The mean flight time increase for MRC optimization is 152 seconds, about 2.5 minutes. The time penalty distribution for MRC includes many flights with more than 5 minutes of cruise time penalty on account of speed changes.

The average time increase due to LRC speed optimization is 3 seconds, amounting to essentially no change from the baseline flight time. The distribution indicates that about half of flights have faster flight times and half of flights have slower flight times due to full LRC implementation, resulting in no appreciable net system delay increase. Very few flights experience a flight time penalty greater than five minutes from LRC optimization.

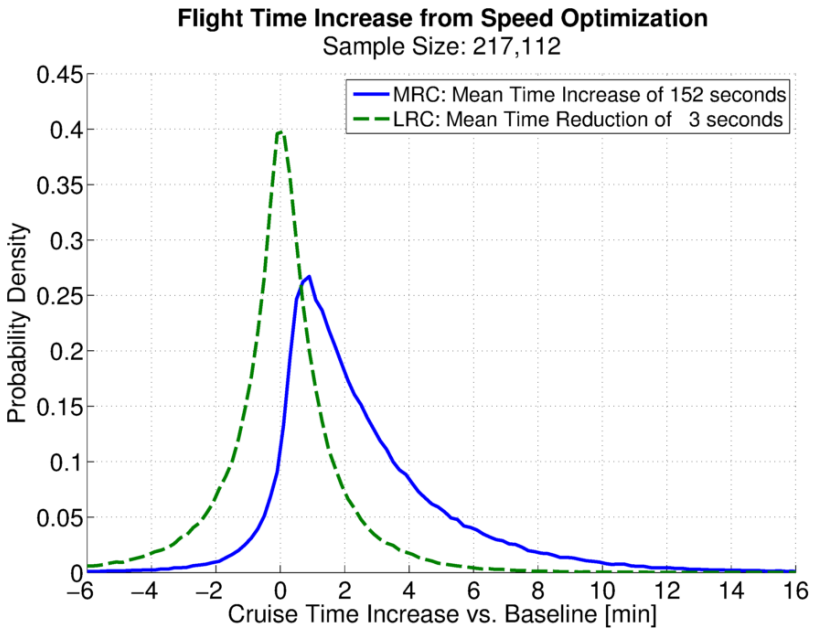

Figure 47. Impact of speed optimization on average flight time

Table 5 provides a summary of fuel burn reduction potential from speed optimization aggregated by stage length. The shortest stage lengths have greatest percentage benefits, with gradually reducing fuel burn reduction by percentage with increasing range. This means that aircraft operating shorter flights operate faster (relative to optimal) than those operating longer flights. Absolute fuel burn reduction increases with longer stage lengths due to greater total trip fuel burn. The impact of stage length on percentage optimization potential is not as pronounced as it was for altitude optimization.

Table 5. Aggregate Speed Optimization Results

Stage Length	Mean Cruise Fuel Burn Reduction		
	MRC	**LRC**	**LRC or Actual[‡]**
0-500 nm	33 lbs	18 lbs	21 lbs
n=67,486	2.22%	1.20%	1.43%
500-1000 nm	95 lbs	49 lbs	58 lbs
n=109,971	2.09%	1.08%	1.27%
1000-1500 nm	205 lbs	92 lbs	113 lbs
n=24,757	1.82%	0.81 %	1.00%
1500-2000 nm	323 lbs	138 lbs	172 lbs
n=9,837	1.74%	0.75%	0.93%
2000-2500 nm	412 lbs	158 lbs	216 lbs
n=4,491	1.59%	0.61%	0.83%
Total	**105 lbs**	**51 lbs**	**61 lbs**
	1.94%	**0.93%**	**1.13%**

4.2.3 DIFFERENCES BETWEEN AIRLINES AND AIRCRAFT TYPES

Differences in speed optimality between airlines can illustrate differences in current operating practices and help identify potential high-benefit operations. Figure 48 shows the speed efficiency performance for the ten airlines with the highest flight count in the output set.

There are several clear trends in this data. First, unlike the altitude optimization case, regional airlines do not all operate farther from optimal speed than mainline carriers. Airline 8 (a regional carrier) has the most efficient speed performance of any airline shown on the figure, while Airline 6 (a mainline carrier) has the least efficient performance. All of the airlines except Airline 6 and Airline 7 have efficiency peaks between 0% and 1%, indicating that the majority of flights at most airlines operate with consideration for speed efficiency. Airline 6 and Airline 7 have much wider distributions of speed performance, with the highest portion of flights occurring at speeds more than 2% below optimal efficiency. This likely indicates airline operational policy rather than airport or aircraft type impacts.

Figure 49 shows the speed efficiency performance for the ten aircraft types with the highest flight count in the output set. As was suggested by the airline decomposition, there is no systematic difference in speed optimality based on whether an aircraft is a regional jet or

[‡] In 38.5% of cases, an LRC speed profile causes an increase in fuel consumption relative to the baseline. That is, many flights were already operated at speeds more efficient than LRC. This column represents the case where all flights already more efficient than LRC maintain the as-flown speed profile, while those that benefit use LRC speed.

mainline aircraft. The aircraft that operated closest to optimal speeds throughout the sample set was the A319. The E145 has the highest portion of flights operating far from optimal.

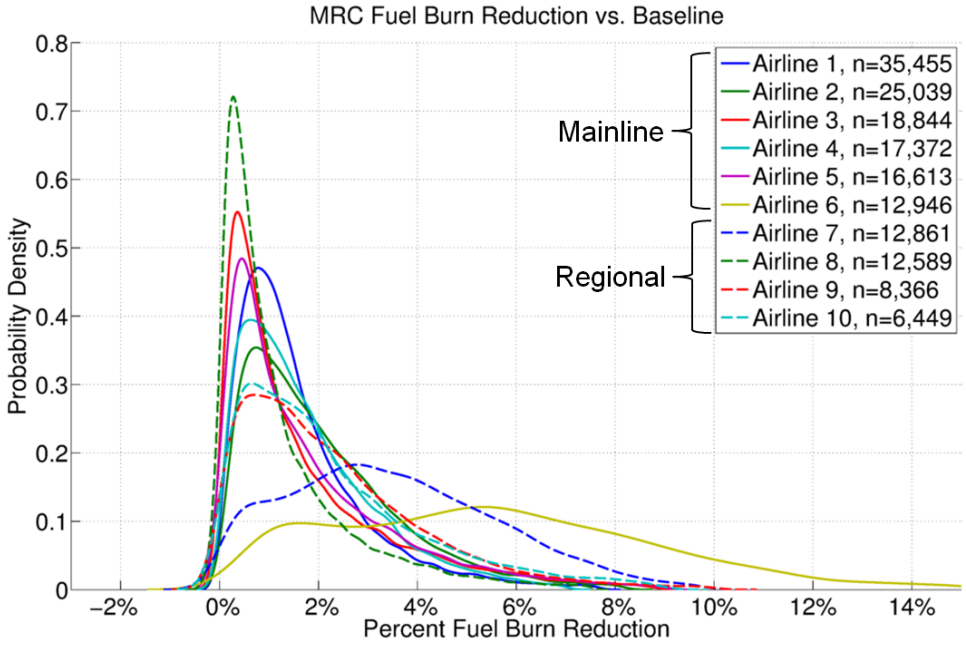

Figure 48. Distribution of benefits from MRC speed optimization for the 10 most common airlines in the output set

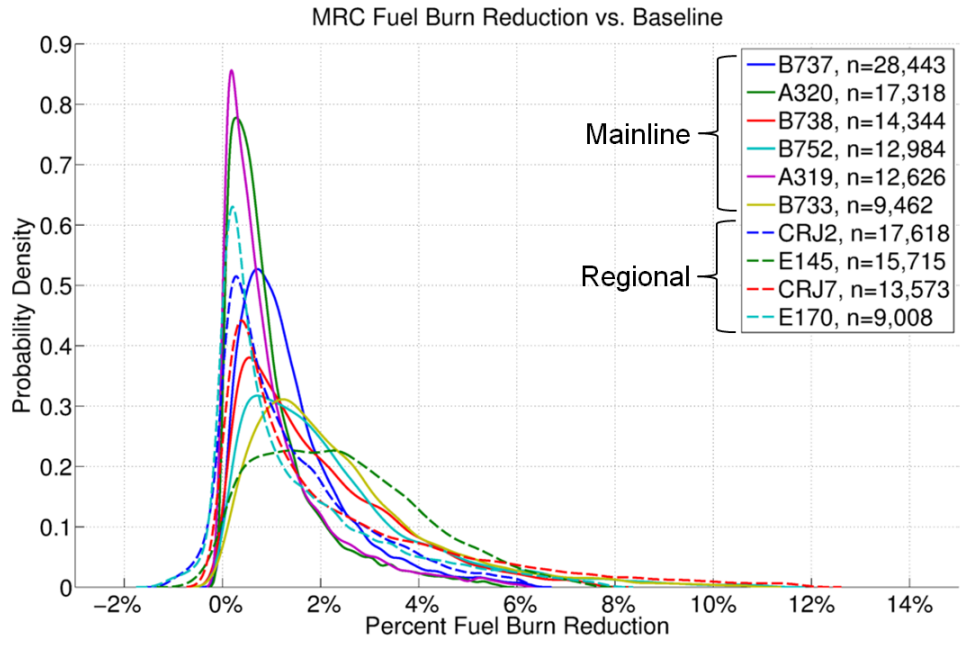

Figure 49. Distribution of benefits from MRC speed optimization for the 10 most common aircraft types in the output set

4.3 Combined Altitude & Speed Optimization Results

Combining altitude and speed into a single optimized trajectory does not have the same benefit of the sum between altitude and speed optimal results on that same flight. This is because the altitude and speed optimal operating point for a given weight and weather condition shifts depending on constraints (as shown in Figure 22 and Figure 28). Regardless on the exact geometry of the fuel efficiency surface for an aircraft, the expected benefits from joint altitude and speed optimization are always expected to be greater than the benefits of speed or altitude optimization alone.

Figure 50 shows the distribution of optimization benefits from joint altitude and speed optimization applied across all flights as described in section 3.9. The mean fuel burn reduction potential is 3.71% with a median of 3.46%. The 25% of operations with highest benefits all have greater than 7.58% fuel reduction potential from joint altitude and speed trajectory optimization.

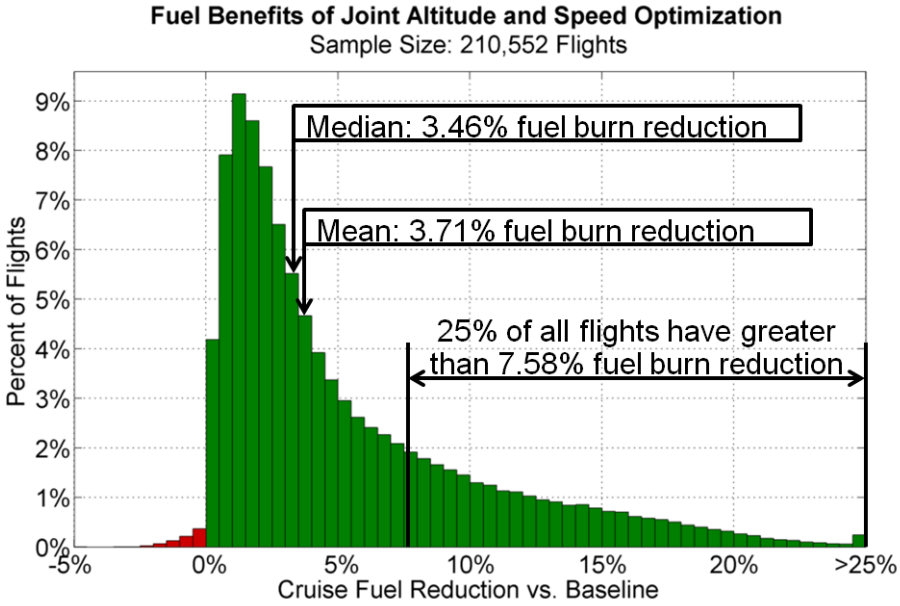

Figure 50. Aggregate fuel burn reduction from joint altitude and speed optimization

The benefits distribution for joint optimization is also different from the altitude and speed distributions in that the most common fuel burn reduction potential is shifted toward higher benefits. That is, eliminating speed and altitude constraints results in fewer flights with very small optimization potential. This indicates that the vast majority of flights have potential benefits from CASO if procedures are put in place that allow for optimal altitude selection accompanied by speed changes. While the joint altitude and speed optimal profile calculated here is essentially a hybrid of the flexible VNAV and MRC speed optimization, similar procedures with LRC speed optimization could be implemented for time-sensitive flights with about 1% less fuel burn reduction.

4.4 Comparison of Speed and Altitude Optimization

The average benefit of either MRC speed optimization or flexible VNAV altitude optimization across all domestic operations in the NAS is on the order of 2% when the respective optimizations are applied independently.

Comparing across the full results set on a flight-by-flight basis, the potential benefits of altitude optimization can be compared to those for speed optimization. Figure 51 shows a comparison of MRC speed optimization and flexible VNAV altitude optimization. The figure shows that 50.5% of flights have more potential benefit from speed optimization while 48.8% of flights have more potential benefit from altitude optimization. 0.7% of flights have equivalent benefits from altitude and speed optimization, or no benefit from either. Therefore, on face value it is difficult to determine whether average US domestic operations need to focus on improved altitude or speed assignment since about half of flights benefit from one over the other.

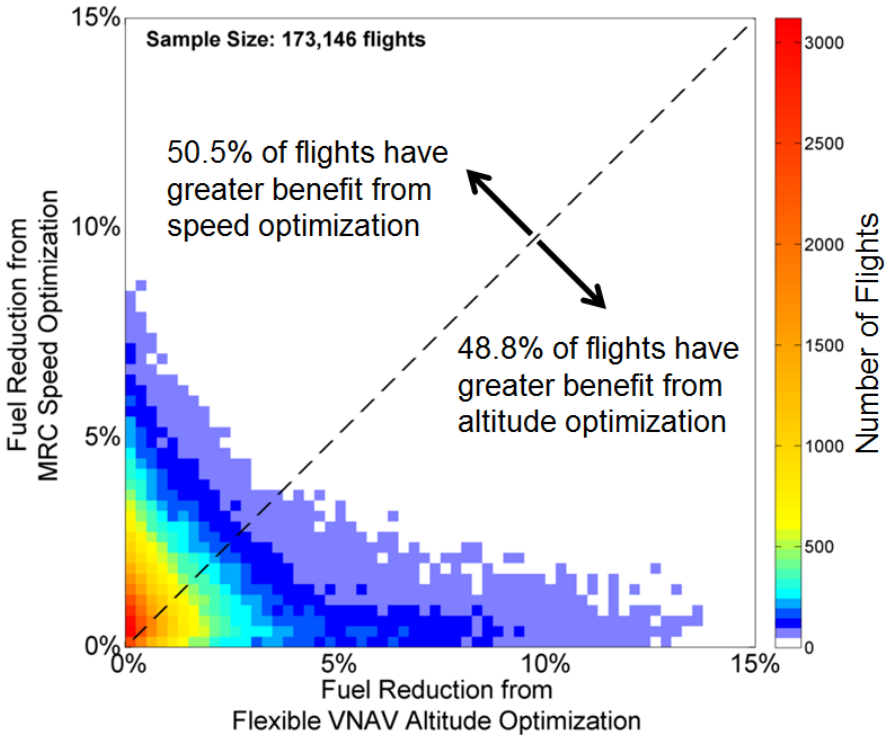

Figure 51. Comparison of optimization potential from altitude vs. speed for all flights in the sample set

The comparison between speed and altitude optimization benefits shown in Figure 51 illustrates some additional aspects of system behavior. The asymmetric hotspot near the lower-left corner of the plot corresponds to the majority of flights in the system. The flights represented by the blue areas are essentially off-optimal outliers. With reference to the high-density area of the plot, most flights skew toward speed benefits. That is, given an average flight

already operating near optimal speed and altitude, the larger gain tends to be possible through speed adjustment. However, amongst the outlier operations, the flights operating far from the optimal altitude profile appear to have more to gain than those operating far from the optimal speed profile (indicated by the wider distribution of off-optimal altitude operations clustered along the bottom of the figure). In short, average flights appear to see greater benefit from speed optimization, while the least-efficient outlier flights can be attributed to altitude inefficiency.

Page Intentionally Left Blank

Chapter 5 DISCUSSION

5.1 Altitude Discussion

5.1.1 ALTITUDE SENSITIVITY VARIATION BY AIRCRAFT TYPE

From the results of the altitude analysis, it was clear that differences between aircraft types played a role in different efficiency outcomes. Certain aircraft types appeared to be more sensitive than others to changing aircraft weight and weather conditions. On the altitude efficiency heat maps, this was shown by the varying width of the optimal altitude window between different aircraft types. Understanding altitude sensitivity by aircraft type is important from an ATC implementation standpoint. ATC and pilots would be able to make better decisions on altitude request prioritization by understanding the differences in sensitivity between flights as well as the optimal altitudes.

In order to characterize and rank the altitude sensitivity by type, a representative metric can be defined for the height of the optimal altitude sensitivity range. This metric, referred to as the "1% optimal altitude window", measures the range of available altitudes where SGR is greater than 99% of the maximum possible value. This range of altitudes is calculated assuming absolute optimal cruise Mach and 75% useful loading of the aircraft, where the useful load is the legal maximum combined weight of fuel, crew, and payload that can be carried by an aircraft. This metric corresponds to the height of the dark blue optimal altitude tunnel shown on the altitude efficiency heat maps under calm-wind conditions. Figure 52 shows two representative "1% altitude efficiency windows" for different aircraft types under these conditions.

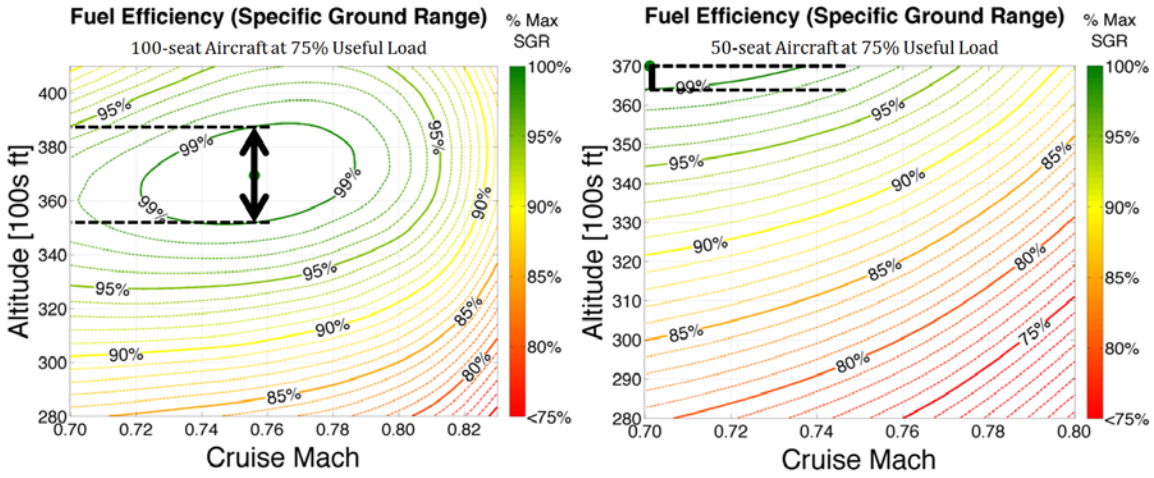

Figure 52. Example 1% altitude efficiency window calculation for two different aircraft types at 75% useful load

The 1% altitude efficiency window can then be used to rank aircraft types by their sensitivity to altitude selection. This ranking is shown in Table 6, ordered by most sensitive to least sensitive.

Table 6. Ranking of aircraft types by 1% altitude efficiency window

75% Load Altitude Sensitivity Rank	Aicraft Type	1% Altitude Efficiency Window [ft]
1 (most sensitive)	E135	677
2	E145	823
3	E45X	823
4	DC91	1195
5	CRJ2	1479
6	CRJ1	1481
7	MD87	2407
8	A321	2699
9	A319	2816
10	A318	2837
11	B738	2878
12	A320	2953
13	B712	2953
14	CRJ7	2969
15	B739	2997
16	A310	3095
17	B737	3097
18	E190	3272
19	A332	3362
20	A333	3395
21	B732	3432
22	B753	3454
23	MD90	3462
24	B77L	3525
25	B734	3539
26	B752	3544
27	B773	3550
28	CRJ9	3586
29	MD82	3586
30	MD88	3586
31	E170	3591
32	A306	3706
33	B735	3724
34	DC93	3728
35	DC10	3771
36	MD83	3830
37	B733	3876
38	B764	4109
49	B762	4167
40	B763	4289
41	B772	4336
42	MD11	4369
43	B744	4634
44 (least sensitive)	B722	4936

Regional Jet (<100 seats)
Narrowbody
Widebody

This listing shows that the range of altitude sensitivity is quite large. Smaller regional jets at 75% useful load generally have an optimal altitude at their service ceiling. This reduces the altitude efficiency window because the only altitudes available within the 1% window are below the optimal altitude (by definition, an aircraft cannot cruise above its service ceiling). The range in 1% altitude efficiency window height ranges from the smallest value of 677 ft for the ERJ-135 to nearly 5000 ft for the B727-200.

An alternative method for analyzing the relative altitude sensitivity of aircraft types is to determine the range of altitudes corresponding to an absolute change in SAR rather than a percentage of efficiency falloff. This accounts for differences in fuel burn between large and small aircraft (1% fuel burn reduction in a B747-400 results in much greater savings than 1% fuel reduction in a CRJ-200). Therefore, Table 7 shows the ranking of altitude efficiency window

size by absolute SAR falloff. The height given in the table represents the range of available altitudes in which an aircraft's SAR is within 0.25 nm/lb of the optimal value. The table shows the maximum possible altitude change by each aircraft type that results in this same total SAR reduction. Again, some of the regional jet aircraft appear high on the sensitivity rankings due to the colocation of optimal altitude and service ceiling.

Table 7. Ranking of aircraft types by 0.25 nm/lb (SAR) altitude efficiency window

75% Load Altitude Sensitivity Rank	Aircraft Type	0.25 nm/lb Altitude Efficiency Window [ft]
1 (most sensitive)	DC91	2135
2	E135	2234
3	E145	2321
4	E45X	2321
5	B773	2865
6	B77L	2906
7	DC10	2925
8	MD87	3057
9	B744	3209
10	A310	3239
11	A333	3282
12	A332	3315
13	MD11	3484
14	A306	3566
15	A321	3625
16	A319	3768
17	A318	3775
18	B772	3896
19	B764	3999
20	MD82	4052
21	MD88	4052
22	B753	4110
23	MD90	4209
24	B712	4242
25	B739	4250
26	B738	4251
27	B763	4254
28	B762	4315
29	A320	4431
30	B752	4443
31	CRJ1	4670
32	CRJ7	4712
33	CRJ2	4829
34	B737	4918
35	B732	4940
36	MD83	4990
37	DC93	5107
38	B734	5267
49	B722	5268
40	B733	5330
41	E190	5346
42	B735	5458
43	E170	5464
44 (least sensitive)	CRJ9	6485

Regional Jet (<100 seats)
Narrowbody
Widebody

From a practical standpoint, Table 6 and Table 7 are interesting because they can help prioritize altitude request in congested airspace. When two aircraft request an altitude change for efficiency reasons but airspace congestion prevents ATC from granting both, differences between aircraft altitude sensitivity could help priorities the requests. If equitable cost reduction across all airlines (regardless of aircraft size) was the objective, the 1% altitude window would be most appropriate for ranking requests. If total system fuel reduction was the objective, the 0.25 nm/lb altitude efficiency window would be the preferred metric.

5.1.2 STEP CLIMB VS. CRUISE CLIMB

It is important to note that all of the altitude optimization methods resulted in average fuel burn reduction potentials between 1.75% and 1.96%. This represents a difference of only 11 lbs in incremental fuel savings per flight by moving from 2000 ft step climbs (the worst performing optimization) to flexible VNAV profiles (the best performing optimization). This suggests that the majority of the benefit from altitude optimization comes from getting close to an ideal trajectory. Fine-tuned refinement of the chosen altitude trajectories provided average benefits on the order of two gallons per flight above what was possible with 2000 ft step climbs. In essence, as long as an altitude trajectory is roughly inside the 1% optimal altitude tunnel illustrated on the altitude efficiency heat maps, fuel efficiency improvement can be substantial compared to baseline profiles.

This is an important finding because basic altitude trajectory improvements, such as improved step climb scheduling, can be implemented in today's NAS without significant investment in new infrastructure or procedures. It is commonly assumed that a constant rate-of-climb trajectory will minimize fuel consumption over the cruise segment of a flight, so there have been suggestions of cruise-climb enabled domestic airspace in next generation enroute structures. The expense and complexity of such a system would be significant due to increased altitude crossing and separation monitoring requirements. More advanced trajectory concepts, such as dynamic climbs or descents in response to weather conditions would require significantly more effort and investment on the part of airlines, pilots, and ATC. The results of this study provide very little motivation for introducing the complexity of cruise climbs or more complicated solutions relative to well-designed step climb procedures.

5.1.3 REGIONAL AIRLINE PERFORMANCE

A key factor in the output dataset for altitude optimization is that short-range and regional operations have far worse altitude efficiency than longer flights. The altitude efficiency benefits for flights less than 500nm were on the order of 5.8% on average across all flights, far greater than the overall average benefits of 1.9%. This disparity points to operational inefficiencies in short range operations with potentially large improvement potential.

Altitude efficiency may be poor on short-range flights for multiple reasons. Many of these flights are operated by regional jet aircraft such as the CRJ-200 and ERJ-145. The optimal altitudes for these aircraft correspond to their service ceilings at FL410 and FL370, respectively. However, on short flights there is less motivation to climb to high flight levels given the normal brevity of the cruise phase. Climbing and descending flights must be separated from other traffic at each crossing altitude. On short flights in congested airspace, this can add significant air traffic controller workload relative to clearing the flights to a lower, less-efficient cruise altitude. Short range flights do not require complicated optimal altitude profiles – normally a single altitude throughout cruise closely approximates the optimal option. Therefore, finding a way to clear more short-range flights closer to optimal operating altitudes could save fuel on the order of 85 lbs per flight.

5.1.4 Operational Considerations and Barriers to Implementation

One of the important drivers of inefficient operations are improperly-timed climbs and descents in the cruise environment. Optimal altitude profiles may include both climbs and descents, depending on the weather conditions along the route of flight. Therefore, accurate and timely weather information is a vital pre-requisite for effective altitude planning and inflight execution. If pilots are provided with high-quality wind field data, aircraft performance information is readily available to determine optimal altitude selection. With the understanding that this optimal altitude may be either above or below the current cruise flight level, pilots could maximize potential fuel savings. In addition, ATC must be able to communicate to pilots when alternative flight levels are available given sector congestion and downstream considerations. This combination of information and communication allows for enhanced altitude efficiency with minimal implementation cost.

In order for ATC and pilots to work more closely on assigning optimal altitudes, ATC will require better information about optimal altitude profiles for each flight. In today's system, flight plans filed with the FAA only provide the initial cruising altitude for each flight. All altitude changes for the remainder of the flight, even when they are included in the detailed printed flight plan used by the pilots, cannot be anticipated by controllers unless communicated by the crew.

5.2 Speed Discussion

5.2.1 Airline-Specific Performance

The differences in speed efficiency profiles between carriers that are shown in Figure 48 suggest that different airlines value fuel efficiency quite differently. The airlines that tend to operate faster than optimal may do so for a variety of reasons including airline schedule constraints, flight planning procedures, and perceived competitive advantage from faster flight times. However, the incremental fuel cost impact of such policies appears to be between 5-10% per flight.

The high-benefits tail of the speed optimization distribution appears to be driven by airline policy more than ATC procedures or pilot preference. Therefore, in an attempt to mitigate cruise fuel consumption, the best place to start is likely with airline flight planning, operations, and scheduling departments.

5.2.2 Potential Applications for Ground Delay Programs

One potential application for MRC speed profiles is in the creation and execution of Ground Delay Programs (GDPs). GDPs are a type of traffic management initiative used to restrict the arrival rate at airports with reduced capacity due to weather, construction, or other conditions requiring intervention. The objective of a GDP is to absorb delays on the ground rather than in the air when delays are inevitable. In current practice, this is accomplished by adjusting the

proposed arrival time of inbound flights so that the inbound rate matches projected capacity. Then, based on the nominal flight time, an expected departure clearance time (EDCT) is issued to each impacted flight. Flights must wait on the ground at the point of departure until the EDCT.

This concept does not currently encourage fuel-optimal behavior. Once a flight is airborne, it is possible to increase speed in an attempt to reduce the arrival delay, thus decreasing fuel efficiency. Given that a flight that has been issued a GDP incurs time costs regardless of departure time, there may be benefit to adjust EDCT calculation procedures such that fuel-minimal speeds are assumed rather than nominal flight times [17]. Pilots assigned an earlier EDCT would then fly an MRC profile. As shown in this thesis, expected fuel consumption for flights impacted by a GDP would average about 1.9% less than baseline operations. The required shift in EDCT time would be on the order of 2.5 minutes across all operations. The greatest challenge in such a concept would be enforcing compliance with MRC speed profiles by participating airlines.

5.2.3 MITIGATION FOR EARLY ARRIVALS

Airline schedules are developed based on a distribution of historical flight block times. Block times are highly stochastic. Therefore, when a flight departs on time or early and does not encounter delays enroute, it may arrive at the destination airport early. This can pose challenges for airlines due to limited gates, personnel, and resources at an airport. Therefore, another potential application for MRC speed optimization is for situations where an enroute flight is projected to arrive early. Rather than continue at normal speeds to face potential gate conflicts and ground delays due to an early arrival, it may be possible to extend the flight time and save fuel costs by reducing speed to MRC.

Chapter 6 CONCLUSION

The purpose of this research was to establish the fuel efficiency benefits pool for cruise speed and altitude optimization in high-altitude domestic airline operations within the CONUS. This was accomplished by building a custom flight profile analysis routine that examined historical radar tracks – corrected for actual weather – using an aircraft point-performance model integrated across each flight. 19 full days of ETMS radar tracks were included in the analysis, resulting in a sample size of 217,000 flights. Each flight's cruise segment was analyzed individually to determine baseline, speed-optimal, altitude-optimal, and joint speed/altitude-optimal profiles and the expected fuel impact of each.

Results indicate potential average fuel savings on the order of 2% for both altitude and speed optimization, and nearly 4% for simultaneous altitude and speed optimization. The aggregate results align well with prior, lower-fidelity modeling of the CASO concept by Lovegren [8]. These are significant fuel savings on a system level, especially given the conceptual simplicity of implementation – if every airplane changed altitude and/or speed slightly, fuel savings amounting to hundreds of millions of dollars could be realized in domestic US operations. Of course, actual constraints in altitude selection (such as weather, turbulence, and airspace congestion) and speed selection (airline schedule constraints, time costs, and ATC flow control) prevent universal adoption of optimal profiles. Therefore, the highest-benefit outcome from this research is a focus on policies and procedures impacting those flights operating farthest from optimal to maximize system fuel benefit.

Stakeholder engagement is a requirement for full understanding of the drivers causing these highly-inefficient outlier operations in today's system, so outreach and engagement with both airlines and ATC will be important for future extensions of this work. Without input on operational constraints and cost structures, it is difficult to draw conclusions about the cause of certain inefficient system components. The altitude inefficiencies in short-range and regional jet operations are an example of an area requiring stakeholder input – while it is clear that there is a systematic reduction in efficiency for these types of flights, the drivers of such behavior are difficult to determine from the data.

Even without stakeholder engagement, there are key outcomes suggested by this study. First, it is evident that most flights (especially at the mainline airlines) are already operating close to optimal altitude and speed profiles. This is reflected in the strong peaks in the 0-2% region of the optimization potential distributions. These flights have the potential for a marginal improvement in fuel performance. However, those flights in the high-benefits tail that currently operate far below optimal altitude or far faster than optimal should be observed more closely for improvement opportunities.

A second key outcome from this study is that optimal altitude efficiency profiles vary significantly based on weather conditions, aircraft types, routes, and other factors. Therefore, altitude trajectory planning requires flexibility on a flight-by-flight basis to achieve maximum benefit. It was also shown that the range of altitudes at which an airplane can operate within 1% of optimal is normally several thousand feet. While operating farther from optimal leads to rapid efficiency falloff, the suggestion of these relatively forgiving "altitude efficiency tunnels" is that flying in the vicinity of optimal altitude is enough to see the majority of the benefit. For example, the incremental improvement of flying cruise climbs compared to well-designed step profiles is shown to be negligible. This is an encouraging results from an implementation perspective because the complexity of cruise climb procedures in the NAS are prohibitive compared to better utilization of the RVSM altitude framework already in place.

6.1 Future Research

There are several potential directions for future research on this topic. First, implementation strategies will be devised for both speed and altitude optimization in domestic operations. Stakeholder engagement on the part of airlines, air traffic controllers, and researchers will be key to leverage analytical results into meaningful operational procedures. Implementation of optimized procedures can occur at the level of the cockpit, airline dispatch facility, or air traffic control center. The technical difficulty, expense, and expected benefits for any implementation strategy depends on the current level of optimality in the system and the reason for that level of optimality. Therefore, some operators may be able to implement changes rapidly to generate large improvements in altitude efficiency, while others may already expend significant resources on the issue and see only marginal gains. Increased collaboration with industry stakeholders will shed new light on the practical benefits expected from speed and altitude optimization.

Second, there are likely applications for CASO concepts in certain international and overwater operations where stage lengths are longer and surveillance systems are less capable than in domestic operations. Analysis of system characteristics and current operating efficiency levels in these systems, including the North Atlantic, West Atlantic, and Pacific Ocean overwater tracks, could assist development and benefits analysis for updated speed and altitude procedures.

Finally, this thesis has focused on applications of optimal trajectory design in today's National Airspace System. As the FAA moves toward modern infrastructure, technology, and procedures through NextGen, it will be important to explore ways in which fuel efficiency can be incorporated into new trajectory planning and control programs. Reduced environmental impact is one of the stated goals of NextGen, so maximizing the efficiency of infrastructure and aircraft through cruise altitude and speed optimization should play an important role.

Chapter 7 BIBLIOGRAPHY

[1] P. Belobaba, A. R. Odoni, and C. Barnhart, Eds., *The Global Airline Industry*, vol. 23. John Wiley & Sons, 2009.

[2] Research and Innovative Technology Administration and B. of T. Statistics, "TranStats," 2014. [Online]. Available: http://www.transtats.bts.gov/. [Accessed: 01-May-2014].

[3] International Air Transport Association, "IATA Fact Sheet: Fuel." 2013.

[4] R. Kar, P. A. Bonnefoy, and R. J. Hansman, "Dynamics Of Implementation Of Mitigating Measures To Reduce CO2 Emissions From Commercial Aviation," 2010.

[5] K. B. Marais, T. G. Reynolds, P. Uday, D. Muller, J. Lovegren, J.-M. Dumont, and R. J. Hansman, "Evaluation of potential near-term operational changes to mitigate environmental impacts of aviation," *Proc. Inst. Mech. Eng. Part G J. Aerosp. Eng.*, Jul. 2012.

[6] L. Jensen, R. J. Hansman, J. C. Venuti, and T. Reynolds, "Commercial Airline Speed Optimization Strategies for Reduced Cruise Fuel Consumption," in *2013 Aviation Technology, Integration, and Operations Conference*, 2013, pp. 1–13.

[7] B. M. Yutko and R. J. Hansman, "Approaches To Representing Aircraft Fuel Efficiency Performance For The Purpose Of A Commercial Aircraft Certification Standard," Massachusetts Institute of Technology, 2011.

[8] J. A. Lovegren and R. J. Hansman, "Estimation of Potential Aircraft Fuel Burn Reduction in Cruise via Speed and Altitude Optimization Strategies," Cambridge, MA, 2011.

[9] A. Midkif, R. Hansman, and T. Reynolds, "Air Carrier Flight Operations," no. July, 2004.

[10] B. Roberson, "Fuel Conservation Strategies: Cost Index Explained," *Boeing Aero Magazine*, no. Ci, Seattle, pp. 26–28, 2007.

[11] A. Cook, G. Tanner, V. Williams, and G. Meise, "Dynamic cost indexing - Managing airline delay costs," *J. Air Transp. Manag.*, vol. 15, no. 1, pp. 26–35, 2009.

[12] W. Roberson, R. Root, and D. Adams, "Fuel Conservation Strategies: Cruise Flight," *Boeing Aero Magazine*, Seattle, pp. 22–27, 2007.

[13] L. H. Mutuel and P. Neri, "Initial 4D Trajectory Management Concept Evaluation," in *Tenth USA/Europe Air Traffic Management Research and Development Seminar (ATM2013) Airport*, 2013.

[14] H. H. Hurt Jr., *Aerodynamics for Naval Aviators*, no. January. Navair, 1965.

[15] F. Mesinger, G. DiMego, E. Kalnay, K. Mitchell, P. C. Shafran, W. Ebisuzaki, D. Jovic, J. Woollen, E. Rogers, E. H. Berbery, M. B. Ek, Y. Fan, R. Grumbine, W. Higgins, H. Li, Y. Lin, G. Manikin, D. Parrish, and W. Shi, "North American Regional Reanalysis," *Bull. Am. Meteorol. Soc.*, vol. 87, no. 3, pp. 343–360, 2006.

[16] R. Palacios and R. J. Hansman, "Filtering Enhanced Traffic Management System (ETMS) Altitude Data," *Metrol. Meas. Syst.*, vol. 20, no. 3, pp. 453–464, 2013.

[17] L. Delgado and X. Prats, "En Route Speed Reduction Concept for Absorbing Air Traffic Flow Management Delays," *J. Aircr.*, vol. 49, no. 1, pp. 214–224, Jan. 2012.